This is a repository copy of *Pickering polymerized high internal phase emulsions: fundamentals to advanced applications*.

White Rose Research Online URL for this paper:
https://eprints.whiterose.ac.uk/221046/

Version: Published Version

**Article:**

# Pickering polymerized high internal phase emulsions: Fundamentals to advanced applications

E. Durgut [a,b,*], F. Claeyssens [b,c]

[a] *Department of Genetics and Bioengineering, Alanya Alaaddin Keykubat University, Alanya/Antalya, Turkiye*
[b] *Kroto Research Institute, Department of Materials Science and Engineering, University of Sheffield, Sheffield, United Kingdom*
[c] *Department of Materials Science and Engineering, INSIGNEO Institute for In Silico Medicine, The University of Sheffield, Sheffield, United Kingdom*

## ARTICLE INFO

## ABSTRACT

Pickering-polymerized high internal phase emulsions have attracted attention since their successful first preparation 15 years ago, primarily due to their large pores and potential for functionalization during production. This review elucidates the fundamental principles of Pickering emulsions, Pickering HIPEs, and Pickering PolyHIPEs while comparing them to conventional surfactant-stabilized counterparts. The morphology of Pickering PolyHIPEs, with particular emphasis on methods for achieving interconnected structures, is explored and critically assessed. Lastly, the mechanical properties and diverse applications of these materials are reviewed, highlighting their use as catalytic supports and sorbent materials. The study aims to guide both new and experienced researchers in the field by comprehensively addressing the current potential and challenges of Pickering PolyHIPEs. Once the mystery behind the closed cellular pores of Pickering PolyHIPEs is resolved, these materials are expected to become more popular, particularly in applications where mass transfer is critical, such as tissue engineering.

## 1. Scope of the review

There are several excellent reviews on both polymerized High Internal Phase Emulsions (polyHIPE) [1–3] and Pickering emulsions [4–6] covering basic principles to current trends in the field. However, a review article specifically focusing on Pickering polyHIPEs is currently missing in the literature. Therefore, this review article aims to provide the basic principles of emulsions, high internal phase emulsions (HIPEs), and polyHIPEs. It will then compile reports about Pickering polyHIPEs, investigating their morphology, properties, and applications, and comparing them with conventional polyHIPEs where relevant. Although 'poly' in polyHIPE stands for polymerization, porous materials obtained from HIPE templates without being polymerized are also within the scope of this review and termed as 'HIPE templates'.

## 2. Emulsions

### 2.1. Definitions and nomenclature

Emulsions are biphasic systems formed by dispersing one immiscible liquid within another. The dispersed phase, in the form of droplets, is known as the internal (or dispersed) phase, while the other phase is the continuous (or external) phase. Emulsions can be classified based on factors such as the hydrophilicity/hydrophobicity of phases, the volume fraction of the internal phase, and the type of stabilizer used. Water-in-oil (w/o) emulsions involve dispersing the internal water phase in a continuous oil phase, while oil-in-water (o/w) emulsions are the opposite (Fig. 1A, B). Emulsions can also be oil-in-oil (o/o) or water-in-water (*w*/w). Based on the volume fraction of the internal phase, emulsions fall into three categories: low internal phase emulsion (LIPE) for <30 % internal phase, medium internal phase emulsion (MIPE) for 30–74 %, and high internal phase emulsion (HIPE) for >74 % (Fig. 1A, C) [7,8]. Furthermore, emulsions can be classified according to the type of stabilizer used—either surfactants or colloidal particles. If the stability is achieved through surfactants, they are termed conventional emulsions. Alternatively, if colloidal particles stabilize the emulsion, it is referred to as a Pickering emulsion (Fig. 1 A, D). Emulsions stabilized by both surfactant and colloidal particles are termed dual emulsified emulsions.

### 2.2. Stabilization of emulsions

An immiscible liquid can be dispersed within another immiscible

---

liquid under shear. When the applied shear is sufficiently high, the internal phase breaks up into droplets within the continuous phase. As emulsion droplets form, the total interfacial area, and consequently, the total interfacial energy, increase within the system. When shear is removed, the dispersed emulsion droplets start to coalesce to reduce the elevated total interfacial energy, ultimately leading the two emulsion phases to separate back into their initial bulk forms. Therefore, to achieve kinetically stable emulsions, emulsion stabilizers are necessary to prevent droplet coalescence.

Conventionally, emulsions are stabilized by surfactants—amphiphilic molecules with both hydrophobic and hydrophilic parts. Due to their amphiphilic nature, surfactant molecules migrate from the generally dissolved continuous phase to the oil/water interface, where the hydrophobic and hydrophilic parts submerge in the oil and water phases, respectively. The type of surfactant determines the type of emulsion formed, either oil-in-water (o/w) or water-in-oil (w/o). Hydrophilic-Lipophilic Balance (HLB), a function of the weight percentage of the hydrophilic portion of the non-ionic surfactant molecule [9], is used to estimate the suitable surfactant for the desired emulsion type. Adsorbed surfactant molecules at the interface reduce interfacial tension between the bulk phases, lowering the energy needed for droplet formation. Adsorbed surfactant molecules on the droplet surface maintains droplet stability by providing steric and/or electrostatic barrier effect [10]. However, surfactant adsorption and desorption at/from the oil/water interface are in thermal equilibrium, and thus, are affected by thermal fluctuations, leading to a loss of emulsion stability and phase separation.

Solid particles in colloid form are another type of stabilizer gaining attention, dating back to Ramsden's [11] and Pickering's [12] pioneering work in 1907. Unlike surfactants, colloidal particles are not necessarily amphiphilic. However, to obtain a stable emulsion, colloidal particles should be wetted in both phases. Similar to surfactants, the phase in which the colloidal particles are dispersed and wetted the most determines the continuous phase of an emulsion—either o/w or w/o. Similar to the HLB value in surfactants, wettability of particles is used to estimate appropriate particles to stabilize the desired emulsion. Because of being wetted by both phases, Pickering agents are adsorbed at the oil/water interface during emulsification. Emulsion droplets covered with colloidal particles are mechanically protected from coalescence with other droplets. Colloidal particles do not reduce the inherent interfacial tension between two phases; therefore, the formation of emulsion droplets requires higher energy than conventional emulsions. Unlike surfactants, colloidal particles are considered to be adsorbed at the oil/water interface irreversibly [13]. Therefore, long-term emulsion stability is achieved in Pickering emulsions.

Pickering-type stabilizers are considered more efficient than surfactants. The required amount of colloidal particles to obtain stable emulsions is generally less than that of surfactants, in terms of weight percentage. For stable emulsions, full surface coverage of droplets by colloidal particles is not necessary. It was demonstrated that a droplet surface coverage as low as 29 % with Pickering agents is sufficient to obtain stable emulsion droplets [14]. Additionally, insufficiently covered emulsion droplets can experience phenomena only observed in Pickering emulsions: particle bridging, limited coalescence, and arrested coalescence (Fig. 2). It was claimed that stable emulsions can be achieved below 29 % surface coverage as well by particle bridging, which is the separation of two emulsion droplets with a monolayer of particles (Fig. 2B) [15]. Additionally, insufficiently covered emulsion droplets can start to coalesce with each other until sufficient surface coverage is achieved; this phenomenon is called limited coalescence (Fig. 2C). Limited coalescence observed in Pickering emulsion is considered a reason for obtaining a relatively narrow droplet size distribution [16]. Alternatively, two emulsion droplets can start to coalesce, but the coalescence can be arrested by particles collecting at and jamming the coalescing region; this phenomenon is called arrested coalescence or sometimes referred to as partial coalescence (Fig. 2D) [17]. Therefore, stable emulsions can be obtained with a lower concentration of colloidal particles compared to surfactants.

Furthermore, depletion attractions can be utilized to enhance emulsion stability. Depletion attraction is an attractive force that occurs between colloidal particles when they are suspended together with smaller depletant molecules. Depletant molecules surrounding the colloidal particles exert pressure, equivalent to osmotic pressure, onto the colloidal particles. When the depletant molecules are excluded from a region between two colloidal particles, the surrounding pressure onto the colloidal particles results in the attractive force between the colloidal particles [18]. The use of depletion interaction to increase the stabilization of Pickering HIPEs has been shown by Kim et al. in a simple oil-in-water emulsion stabilized by colloidal silica particles, by adding PEG to the water phase (Fig. 3) [19]. It was demonstrated that as long as the depletant molecule (PEG) and the particles (colloidal silica) do not interact with each other strongly and they are well dispersed in the continuous phase, it is possible to obtain a stable emulsion with 90 % internal phase with a surface coverage as low as 6 %.

### 2.3. Destabilization of emulsions

The stability of an emulsion is defined as its resistance against changes in physicochemical behaviour over time [20]. The physicochemical behaviour of an emulsion is related to the interactions between emulsion droplets, significantly influenced by the nature of the stabilizer and the stabilization mechanism. Emulsion destabilization mechanisms include phase inversion, gravitational separation, Ostwald ripening, and coalescence.

Phase inversion results in a change in emulsion type, shifting from o/w to w/o, or vice versa. Gravitational separation arises from the density mismatch between the continuous phase and the internal phase, categorized into creaming and sedimentation. Creaming occurs when the
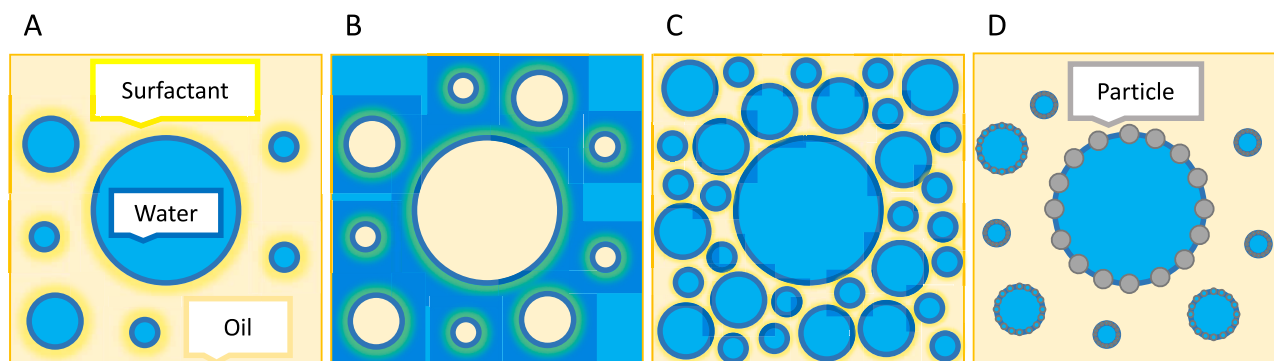


**Fig. 1.** The classification of emulsions. (A) Surfactant-stabilized (conventional), w/o, LIPE (assuming that the internal phase volume is <33 %), (B) o/w counterpart of A, (C) HIPE counterpart of A (assuming that the internal phase volume is >74 %), (D) Pickering counterpart of A.
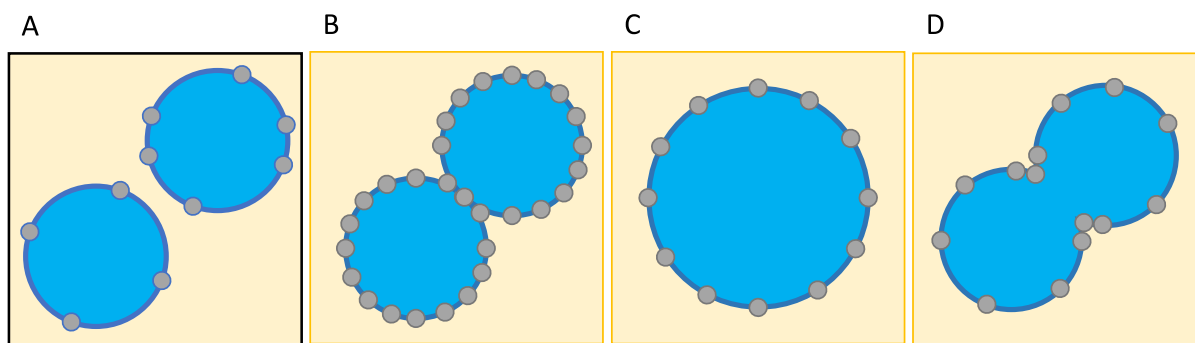
**Fig. 2.** Observed phenomena in Pickering emulsions regarding the efficient stabilization of the emulsion; (A) insufficiently covered emulsion droplets can coalesce via: (B) particle bridging, where two emulsion droplets are separated from each other by the monolayer of particles; (C) limited diffusion where the droplets coalesce until reaching the sufficient surface coverage; (D) arrested coalescence of two emulsion droplets, where droplets start to coalesce but the coalescence is arrested due to particle jamming at the necking region.
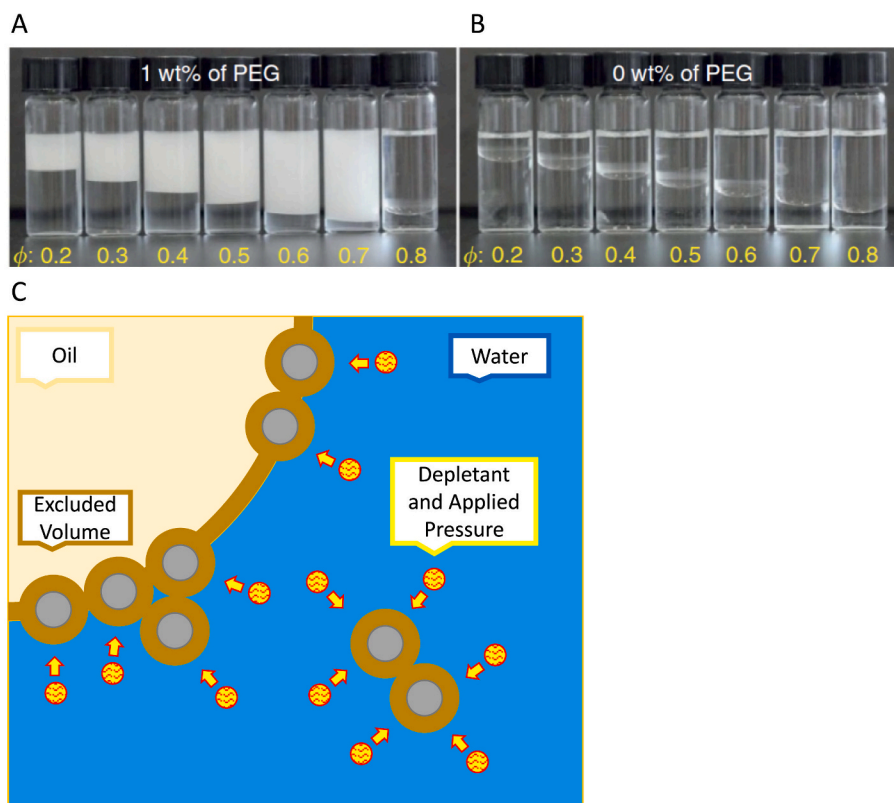


**Fig. 3.** The preparation of emulsion by exploiting depletion attraction: (A) The digital images of formation of Pickering HIPE at various internal phase fraction in the presence of depletant PEG and (B) their phase separated counterparts in the absence of depletant agent. Adapted with permission from [19]. (C) The schematic representation of achieving stability with depletion attraction (redrawn from [19]).
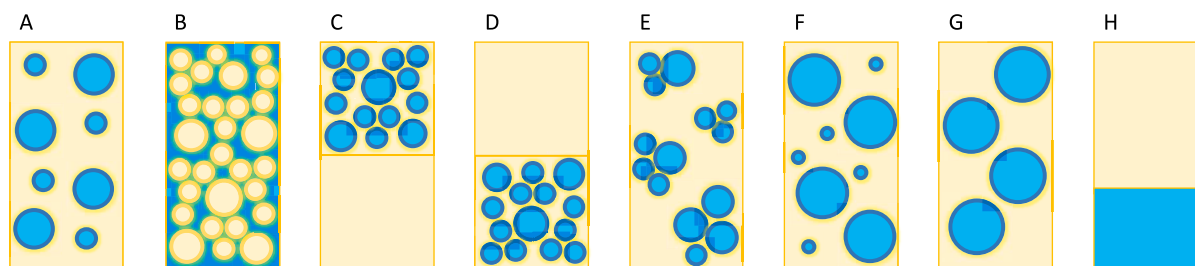


**Fig. 4.** The schematic representation of emulsion destabilization mechanisms; (A) The kinetically stabilized emulsion, (B) emulsion experiencing phase inversion where the internal water phase becomes continuous phase, (C) creaming, (D) sedimentation, (E) flocculation, (F) Ostwald ripening, (G) coalescence and the (H) phase separated emulsion due to emulsion destabilization.

internal phase has lower density, causing emulsion droplets to migrate and accumulate at the top over time, resulting in two phases within the system, with the continuous phase at the bottom, and the concentrated emulsion on top (Fig. 4C). Conversely, in the case of sedimentation, if the internal phase has higher density than the continuous phase, the emulsion droplets accumulate at the bottom (Fig. 4D). When the emulsion droplets aggregate with each other locally, this destabilization is referred to as flocculation (Fig. 4E). This is mainly due to the attractive forces between emulsion droplets such as van der Waals or electrostatic interactions, leading them to cluster [21]. Ostwald ripening is the diffusion of smaller emulsion droplets into the larger ones and mainly stems from the difference in internal (Laplace) pressure of emulsion droplets due to size difference [22]. Therefore, emulsions with broader emulsion droplet size distribution are more susceptible to Ostwald ripening (Fig. 4F). Similarly, coalescence is the merging of emulsion droplets with each other to form larger droplets (Fig. 4G). The mentioned destabilization mechanisms are interrelated, and the occurrence of one can trigger the other destabilization mechanisms as well. Consequently, as the emulsion experiences these processes, phase separation occurs where the continuous and the internal phase are separated completely from each other (Fig. 4H).

Among the mechanisms involved in emulsion destabilization, Pickering emulsions are resistant to coalescence compared to conventional emulsions. Particles are considered to adsorb to the oil/water interface irreversibly since the energy required to remove particles from the interface is a few orders of magnitude higher than the thermal energy [5,23]. Therefore, the emulsion droplets are mechanically shielded by the particles located at the o/w interface forming a physical barrier around emulsion droplets preventing the coalescence of neighboring droplets.

The superior stability of Pickering emulsions can be a problem when the application necessitates a controlled destabilization of the emulsion or when the application results in the production of Pickering emulsion unintendedly as a by-product [24]. Therefore, methods to destabilize Pickering emulsions are also an active area of research. Melle et al. applied an external magnetic field to Pickering emulsions stabilized by magnetic particles, observing that the strong magnetic field de-attaches particles from the oil/water interface to destabilize the emulsion [25]. Similarly, the application of an external electric field was reported to destabilize Pickering emulsions, not by detaching particles from the interface, but by relocating already adsorbed particles on the emulsion droplet so that the droplets can access each other to coalesce [26]. Griffith et al. demonstrated the destabilization of o/w Pickering emulsion by adding more hydrophobic particles to the system, causing oil droplets to preferentially wet the hydrophobic particles rather than maintaining their droplet form [27]. Kumar et al. reported a versatile method to induce destabilization of Pickering emulsions by induced liquid-liquid phase separation due to the addition of a solute which is soluble in both phases of the emulsion [28].

## 3. HIPE

As mentioned in the previous sections, emulsions can be classified based on the internal phase fraction, with High Internal Phase Emulsions (HIPEs) typically defined as emulsions containing over 74 % internal phase. This threshold is derived from the maximum packing density of face-centred cubic, non-deformable monodisperse spheres. Theoretically, beyond a 74 % internal phase fraction, monodisperse spheres are compelled to deform into polyhedra, leading to restricted mobility of internal phase droplets. These alterations are accompanied by changes in the emulsion's physical properties, particularly its rheological behaviour. Thus, the key factor distinguishing HIPEs from emulsions with lower internal phase fractions is the shift in rheological properties. Although this change is generally proportional to the internal phase fraction, a sudden increase in emulsion viscosity can be observed at volumes of internal phase lower or higher than 74 %, given that

emulsion droplets are not non-deformable monodisperse spheres. The HIPE-like behaviour of the emulsion is contingent upon the deformability of the liquids and the polydispersity of the emulsion droplets. Consequently, the definition of HIPEs is a subject of debate, and an alternative definition considers emulsions with an internal phase volume fraction higher than the maximally random jammed packing concentration [29].

HIPEs demonstrate viscoelastic behaviour due to their closely packed emulsion droplets, behaving like a viscous liquid above the applied critical stress (yield stress) and an elastic solid below it [30]. This unique rheological property makes HIPEs suitable for applications such as 3D printing inks [31,32], as they exhibit desirable viscosity and shear-thinning behaviour. Additionally, owing to their self-supporting physical state and high capacity for encapsulating molecules in the internal phase, especially with their high internal phase volume, HIPEs are attractive in the food, pharmaceutical, and cosmetic industries [33]. In the realm of material science, HIPEs serve as templates for producing highly porous materials, a topic that will be detailed in the following chapters.

### 3.1. The HIPE preparation process

Conventional HIPEs have been in use since 1966 [7], but the first successful preparation of Pickering HIPE and its utilization as a template were reported in 2007 first by Colver et al. (through forced sedimentation) [13] and followed by Menner et al. (without forced sedimentation) [34]. The late emergence of Pickering HIPEs can be attributed to a few factors. First, early studies reported an inversion in Pickering emulsions at high internal phase; indeed, in 1999, Binks et al. demonstrated that Pickering emulsions experience catastrophic phase inversion, without any sign of hysteresis during the inversion when the volume of the internal phase reaches ~70 % [35]. This catastrophic phase inversion was demonstrated for both water-in-oil (w/o) and oil-in-water (o/w) emulsions. Additionally, this was supported by a thermodynamic model developed by Kralchevsky et al. in 2005, which predicted catastrophic phase inversion above 50 % internal phase in Pickering emulsions [36]. The difference in proposed internal phase volumes between the experimental (70 %) and predicted model (50 %) was attributed to kinetic effects. On the other hand, advances in material science and chemistry, particularly the fast advance in inorganic nanoparticle manufacture in the early 2000s, likely contributed to the broadening of particle options as a stabilizer. This, in combination with the use of surface modification techniques, enabled obtaining particles with the desired wettability in both phases.

Similar to lower internal phase emulsions, two immiscible liquids, a suitable stabilizer, and mechanical shear are required to form an HIPE. The mechanical shear should be high enough to enable droplet break-up, and the stabilizer should locate themselves fast enough at the newly formed interface to stabilize emulsion droplets before they recoalesce. As the internal phase volume increases within the emulsion, the accompanied increase in viscosity reduces the mixing efficiency and homogeneity. Therefore, droplet break-up becomes no longer possible. Since viscosity is a limiting factor for the preparation of the HIPE, diluent solvents can be used to thin the initial phases of the emulsion [37,38].

Conventionally, the internal phase is added dropwise to the continuous phase under shear to prepare an HIPE (Fig. 5A). Rather than adding the internal phase dropwise, combining all the ingredients in a container followed by simple hand shaking was reported to form an HIPE as well [39,40]. Alternative methods were also reported to obtain HIPEs either by using phase inversion or forced sedimentation (Fig. 5B). Sun et al. reported that it is possible to turn a particle-stabilized oil-in-water low internal phase emulsion (LIPE) into a water-in-oil HIPE via phase inversion by simply changing the pH or salt concentration of the water phase [41]. This changes the colloidal ionizable poly(styrene-*co*-methacrylic acid) particle wettability and the stability of the HIPE. This was
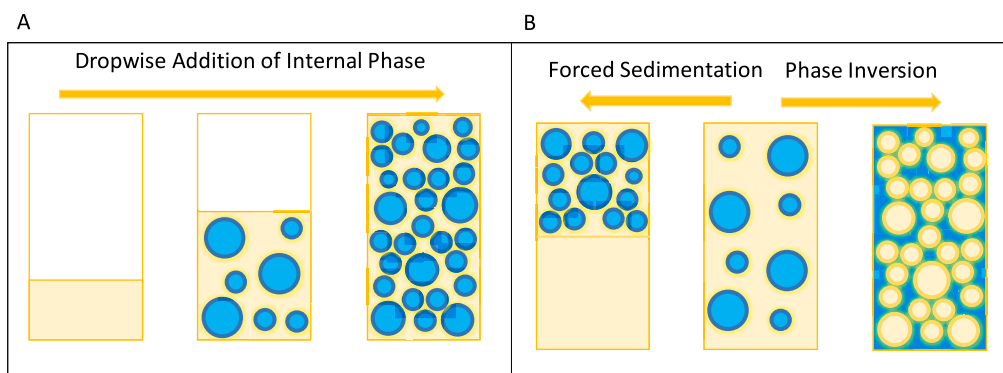
**Fig. 5.** The methods to prepare HIPE is schematically represented: (A) Conventional preparation of HIPE where the internal phase is being added dropwise and slowly while the emulsion is being mixed and (B) the production of HIPE from dilute emulsions either by forced sedimentation or phase inversion.

further illustrated via using other ionizable particles (sulfonated polystyrene) [42] and $CO_2$-responsive block copolymer [43], which wettability can be tuned by either changing the salt/pH and CO2 concentration of the emulsion, respectively, so that the particles favourably stabilize the inverted emulsion. Alternatively, LIPEs or MIPEs can be forced to sediment (i.e., by centrifugation) so that the excess continuous phase is separated from the highly concentrated part of the emulsion [44–46].

### 3.2. Rheology of HIPE

As mentioned in the previous section, (HIPEs) exhibit viscoelastic properties, displaying elastic solid and viscous liquid-like behaviour depending on the applied shear stress. In a wide range of oscillation frequencies, HIPEs exhibit constant elastic and loss modulus, with the elastic modulus being a few orders of magnitude higher than the loss modulus, indicating the viscoelastic behaviour of HIPEs [47]. The viscoelastic properties, including viscosity, elastic modulus, and yield stress, are mainly determined by the interfacial tension between the phases, mean emulsion droplet size and size distribution [48], the internal phase volume, the viscosity of the continuous and internal phase [49] and the inter-droplet interactions [50]. However, the parameters affecting HIPE rheology have a complex and significant effect on each other.

In the case of Pickering HIPEs, they exhibit a higher elastic modulus than that of conventional HIPEs. The increased elasticity of the Pickering HIPEs is attributed to a rigid interfacial layer due to attractive interactions between solid particles (Fig. 6A) [51]. Recently, Kaganyuk et al. revealed the effect of excluded effective internal phase volume due to the size difference between surfactants and colloidal particles (Fig. 6B) and attractive lateral capillary interactions among particles on Pickering HIPE rheology (Fig. 6C, D) [52].

### 3.3. Emulsion droplets of HIPE

Theoretically, polyhedral-shaped emulsion droplets are expected when the internal phase volume exceeds the maximum packing density of monodisperse emulsion droplets. However, droplets can be spherical even at internal phase fractions reaching 90–98.5 % when the emulsion droplets are polydisperse [53,54], as the theoretical maximum packing density of polydisperse spheres can be higher than 74 %. Alternatively, when the emulsion droplets are relatively small and the interfacial tension is high, emulsion droplets resist being deformed into polyhedra due to their high Laplace pressure, the pressure difference between the inside and outside of the droplet [33]. Therefore, the emulsion droplet size and distribution, as well as interfacial tension, are the main parameters determining the emulsion droplet shape in HIPEs.

The droplet size of the final emulsions is mainly determined by the interfacial tension between the phases, induced shear stress during emulsification, internal phase volume, and stabilizer-associated parameters, which will be focused on in this section. In terms of conventional HIPEs, the concentration of surfactant is inversely proportional to the obtained final droplet size [55]. This is mainly due to the reduced interfacial tension parallel to increased surfactant concentration and the abundance of surfactant molecules, allowing a larger interfacial area to be stabilized.

In the case of Pickering HIPE, the emulsion droplet size correlates with the particle size. Levine et al. reported that the particle size should be an order of magnitude lower than the desired final emulsion droplet size [56]. Similar to surfactant, increased particle concentration results in smaller emulsion droplets [57,58]. However, depending on the interactions, either inter-particle or between emulsion phases and particles, a further increase in particle concentration can result in the enlargement of the HIPE droplet size [59,60]. This is due to increased continuous phase viscosity due to being suspended in a higher concentration of particles, therefore increased emulsion viscosity as the
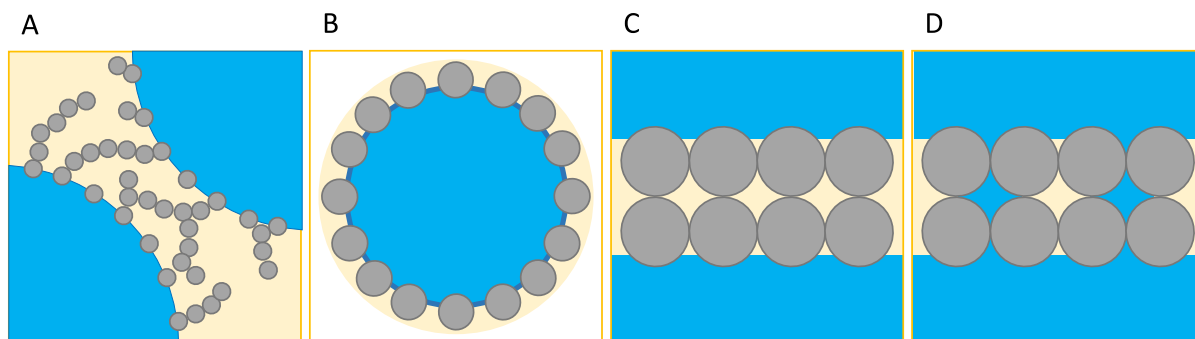


**Fig. 6.** The schematic representation of mechanisms involved in increased Pickering HIPE elastic modulus: (A) Interparticle interaction forming 3D network in interfacial area, (B) excluded volume effect, (C, D) lateral capillary interactions between particles. Figures are redrawn from [52].

internal phase fraction of the emulsion increases. Additionally, particles can flocculate due to inter-particle interactions, leading to a reduction of the effective stabilizer amount in the continuous phase [61]. Overall, a typical Pickering HIPE droplet size is larger than in conventional HIPEs.

## 4. PolyHIPEs

HIPEs can be employed as a template to produce highly porous materials. If the continuous phase of the HIPE consists of polymerizable monomers and in the presence of an appropriate polymerization initiator, the 3D network surrounding the internal phase droplets can be polymerized. Subsequent removal of the internal phase leaves behind porous polymers, where the polymerized continuous phase forms the skeleton of the material, and the internal phase forms the pores (sometimes referred to as voids or cavities). This technique, utilizing HIPE as a template, is known as emulsion templating/HIPE templating. The material obtained via the polymerization of the continuous phase is known as a polyHIPE (Fig. 7). The comparison of conventional and Pickering polyHIPE is presented in Fig. 8.

In conventional polyHIPEs, pores are interconnected through pore throats (sometimes referred to as void cavities or interconnects) on the pore surface. Pore throats, generally proportional to pore size [62], allow mass transfer through the material. Therefore, polyHIPEs find applications in various fields due to their ease of manufacturing, cost efficiency, and tuneable properties such as porosity, pore size and shape, interconnectivity, surface area, and mechanical properties. Additionally, functional polyHIPES can be obtained during the preparation by using functional block copolymers [63]. They are commonly used as catalyst supports [64,65], scaffolds for tissue engineering [66,67], and absorbents [68,69].

There are several concerns associated with conventional polyHIPEs obtained from surfactant-stabilized HIPEs. While polyHIPEs offer versatility during preparations, some of the concerns of a typical conventional polyHIPES are as follows: Firstly, the obtained pore size and pore throat size are small, approximately 10–50 and 1–5 μm, respectively [70,71]. Such small pore size may limit their suitability for 3D tissue culture scaffolds due to restricted cell infiltration. This pore size



**Fig. 8.** SEM Images of typical polyHIPEs obtained by surfactant-stabilized (conventional polyHIPEs) or colloidal particle-stabilized HIPEs (Pickering polyHIPEs). Overall porous structure of a conventional polyHIPE; pores and pore throats are 10 and 1 um, respectively. The orange circle highlights a pore, an imprint of HIPE droplets after being polymerized and internal phase removal. The yellow circle highlights a typical pore throat. Overall porous structure of a typical Pickering polyHIPE with ~100 um pores without interconnecting pore throats. The green circle highlights the thin polymeric film covered pore throats. The orange arrows show the interfacial polymeric film separating two neighboring pores, the green arrow show the pore surface and the yellow arrow show the polymerized trigonal region (Plateau border), the intersect of three pores. (For interpretation of the references to colour in this figure legend, the reader is referred to the web version of this article.)



**Fig. 7.** The digital images of highly viscous, self-supporting HIPE and its optical micrographs (left). The photopolymerized 3D polyHIPE and its SEM image of the internal structure. Scale bars are 200 μm.

allows for cell integration and 3D tissue culture but may impede vascularization when used for implantation, which typically requires pore sizes larger than 100 μm [72]. Controlled destabilization of emulsion droplets before polymerization occurs can be utilized the enlarge pore size and pore throats [73]. Secondly, the use of surfactants increases the production cost of the method, as the surfactant concentration required for producing HIPEs and polyHIPEs is typically high (10–30 wt% of the monomer concentration [74–76]) although there are reports demonstrating <3 % of surfactant can effectively produce HIPE [77,78]. Third, commonly used surfactants are associated with health and environmental toxicity [79]. It is important to note that environmental surfactants are also exist and used to stabilize HIPE, such as polyglycerol polyricinoleate [80–82]. If the final product needs to be cleared from the surfactant, then this can only be achieved in a labor-intensive manner, necessitating the usage of organic solvents. Additionally, even after being washed, the leftover surfactant on the polyHIPE can leach out. The remnants of surfactants also function as a plasticizer, reducing the mechanical properties of conventional polyHIPE [83].

Pickering polyHIPEs offer an alternative to conventional polyHIPEs. Firstly, any surfactant-associated concerns are eliminated. Secondly, larger pore sizes can be obtained with Pickering polyHIPEs. Colloidal particles can add interesting functionalities; they can function not only as HIPE stabilizers but also as crosslinking hubs [84]. Rough pore surfaces can be obtained due to embedded particles within the pore surface, and similarly, these particles can be magnetic [85] or catalytic [86], enabling the production of functional polyHIPEs in a one-pot synthesis. Third, since Pickering HIPEs exhibit superior stability, they can resist destabilization when exposed to polymerization-associated conditions,

such as elevated temperature. However, Pickering polyHIPEs exhibit one major drawback: they do not exhibit pore throats. This drawback eliminates their usage in applications where mass transfer is needed. Therefore, in this section, the morphology and applications of Pickering HIPEs will be reviewed with a focus on the methods to produce inter-connected Pickering polyHIPEs.

### 4.1. Pores

The pore size and distribution of the polyHIPE are mainly deter-mined by the emulsion droplets. Tuning the emulsion droplets would directly affect the pore size and distribution of the polyHIPE. However, the deviation between droplet and pore size can occur during poly-merization. This can be due to changes in emulsion stability depending on the cure rate [87] or due to volume shrinkage either by monomer-to-polymer conversion or capillary stress induced by the drying process of the material [88]. Both conventional and Pickering polyHIPEs can experience the mentioned deviation of droplet to pore size in a similar manner. On the other hand, polymerization can affect the final polyHIPE morphology significantly depending on the type of initiator, in which phase the initiator is dissolved, and/or the partition coefficient of the initiator.

Polymerization of HIPE requires the initiator to be dissolved either in the continuous phase or in the internal phase. When the initiator is dissolved in the continuous phase, the polymerization starts within the polymer phase. However, if the initiator is dissolved in the internal phase, the polymerization starts from the interface, specifically from the continuous phase film surrounding the emulsion droplet. The locus of initiation affects the pore shape, the thickness of the pore walls, and the interconnectivity of the polyHIPE [89]. Continuous phase initiation leads to the formation of spherical and interconnected pores, while interfacial initiation results in polyhedral-shaped closed pores in con-ventional polyHIPEs (Fig. 9).

Traditionally, the morphological difference observed in interfacial initiation is attributed to locking-in the emulsion droplets since the polymerization occurs at the continuous phase films covering the emulsion droplets. As the polymerization continues on the interface, the osmotic pressure difference between the interface and the Plateau border leads to the migration of monomers from the Plateau border to the interface, resulting in a thicker polymer wall separating two emul-sion droplets. Conversely, when the polymerization initiates from the continuous phase, this allows the diffusion of monomers from the

interface to the Plateau border, resulting in a thinner continuous phase film between neighboring droplets that is prone to rupture and allows the formation of pore throats as well [90]. However, emulsion droplets that are originally spherical turn into a polyhedron during interfacial polymerization, rather than keeping their original shape. This is ques-tioned by Koch et al., and the osmotic pressure difference as a mecha-nism to induce polyhedral closed cellular morphology in interfacial-initiated conventional polyHIPE is refuted [91] and a new mechanism explaining the pore shape transition is provided (Fig. 10) [92]. Ac-cording to the mechanism, as the polymerization continues from the interface, the surfactant molecules migrate either to the interface or to the inside of the polymer film where the surfactant is more soluble. This accumulation of surfactant at the interfacial continuous phase leads to an increase in the interfacial area and, therefore, a transition from a spherical to a polyhedral pore shape. Additionally, the surfactant trap-ped inside the polymer film can be washed out, revealing a porous inner layer after production. Although it is an interesting mechanism explaining the pore shape transition during interfacial polymerization of HIPE, the suggested mechanism contradicts with the seminal work of Williams et al. [93]. It was demonstrated that increasing the surfactant concentration above ~7.5 % results in not only interconnected pores but also pore shape transition from polyhedral to spherical when the poly-merization occurred at the interface.

A similar pore shape transition is observed in Pickering polyHIPEs as well. Continuous phase initiation yields a spherical, particle-decorated pore surface. Conversely, the interfacial initiation of polymerization results in polyhedral pores. Additionally, during polymerization, the diffusion of monomers toward the internal phase, in other words, beyond the stabilizing particles located at the oil/water interface, was observed. So that the particles were not observed on the pore surface; instead, particles were trapped in the polymer wall (Fig. 11) [84]. By locating the particles within the polymer, it is possible to hypothesize the monomer diffusion toward the internal phase during polymeriza-tion. It might be the case for conventional polyHIPE as well since it is impractical to observe such a diffusion in conventional polyHIPE, and this phenomenon might contradict the mechanism proposed by Koch et al.

At first glance, the proposed mechanisms may appear contradictory. However, it is important to note that HIPEs are complex systems in which small changes in the components can lead to significant changes in both the HIPE and resulting polyHIPE morphology. Therefore, the observed differences may stem from variations in the HIPE components
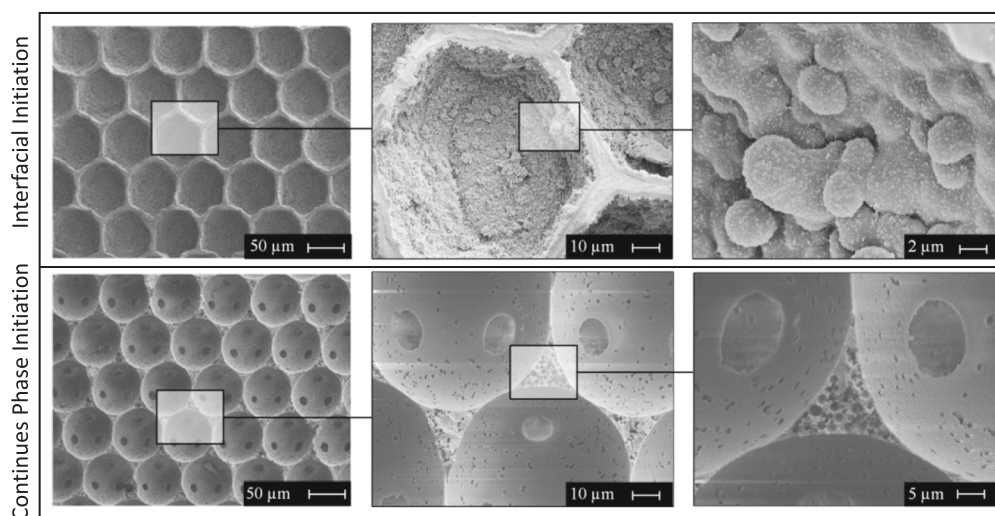


**Fig. 9.** The changes in conventional polyHIPE morphology caused by the difference in locus of initiation; closed polyhedral pores with rough pore surface are obtained in interfacial initiation, while spherical interconnected pores with a smooth pore surface are obtained in continues phase initiation. Adapted with permission from [89]. Copyright 2017 American Chemical Society.
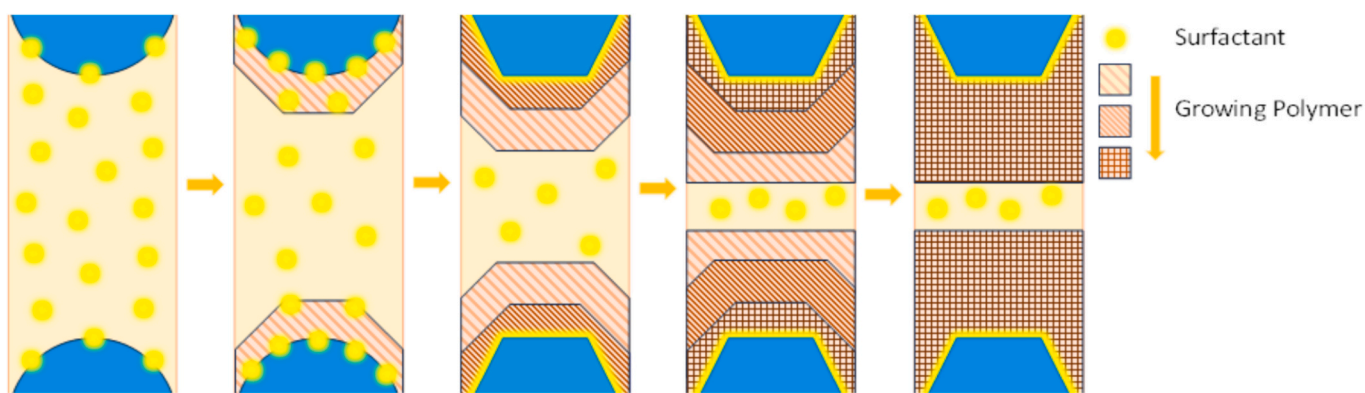
**Fig. 10.** Schematic representation of pore shape changes from spherical to hexagonal in during the interfacial polymerization of HIPE. The figure is redrawn from [92].
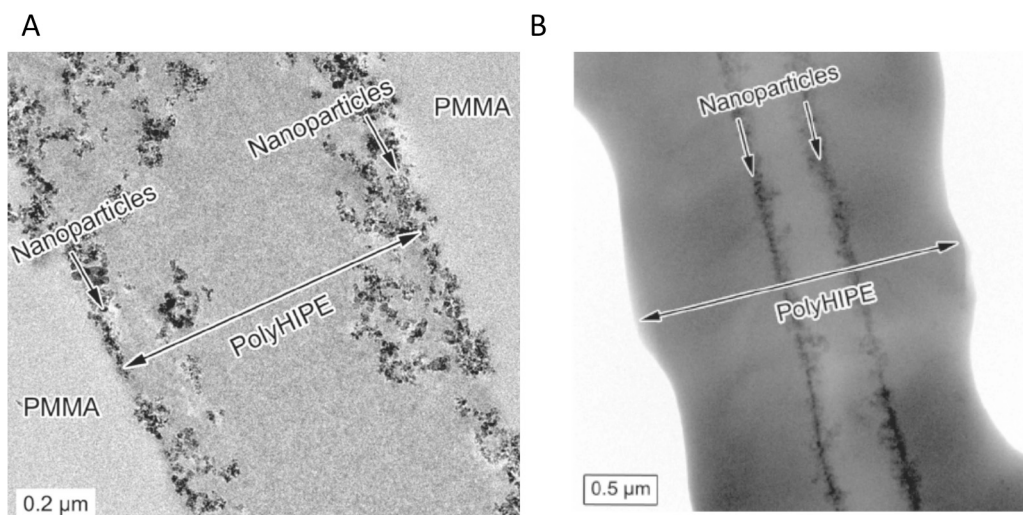


**Fig. 11.** TEM images of polyHIPEs demonstrating the location of particles. (A) Continuous phase initiated polyHIPE where the particles are at the interface, (B) interfacial initiated polyHIPE where the particles are located within the interfacial polymer film due to monomer diffusion toward the internal phase during polymerization. Adapted with permission from [84]. Copyright 2011 American Chemical Society.

rather than conflicting explanations. Additionally, the effects of the initiation locus and stabilizer type on polyHIPE pore shape further complicate drawing a definitive conclusion. In any case, understanding the key factors driving pore shape transitions during polyHIPE preparation requires more detailed investigation and comparison.

Similarly, Kim et al. investigated three photoinitiators, ranging from hydrophobic to hydrophilic as determined by their decane/water partition coefficients, and the light intensity to induce polymerization on both conventional and Pickering polyHIPE morphology [94]. As the hydrophilicity of the initiator increases, the pores of Pickering polyHIPE transform from a spherical to polyhedral shape. In parallel to Gurevitch et al. [84], the diffusion of monomers to the interface was observed when interfacial polymerization occurs; therefore, nanoparticles were embedded within the polymer wall. While the partition coefficient does not affect the interconnectivity of the pores in Pickering polyHIPEs, the pores in conventional polyHIPEs are significantly affected both in shape and interconnectivity as the hydrophilicity of the photoinitiator increases. Additionally, the effect of light intensity on Pickering polyHIPE morphology was insignificant, while a significant effect was observed on conventional polyHIPE, where the open cellular morphology is achieved when the light intensity was high in the interfacially initiated HIPE.

### 4.2. Pore throats

In this section, (i) the prevailing views on pore throat formation in conventional polyHIPEs, (ii) recently proposed pore throat formation mechanisms, (iii) the mechanism behind the closed-cellular morphology in Pickering polyHIPEs and (iv) the methods induce pore throat formation in Pickering polyHIPEs will be reviewed. It is important to note that the pore throat formation in polyHIPEs is a subject still under debate.

#### 4.2.1. The formation of pore throats in PolyHIPEs

Cameron et al. investigated HIPE morphology at different stages of polymerization through CryoSEM. In this study, pore throat formation was observed at the thin interfacial area between two neighboring droplets at the gel point of the HIPE, the transition between viscous emulsion to gel network (Fig. 12A) [95]. Therefore, polymerization-induced volume contraction was proposed as a governing factor of pore throat formation. On the other hand, Menner et al. argued that pore throat formation is primarily caused by mechanical actions during post-synthesis processing, such as solvent washing and drying under vacuum (Fig. 12B) [96]. These processes lead to the rupture of thin polymer films covering the interfaces between neighboring droplets, resulting in pore throats. Menner et al. hypothesized that the formation of pore throats is influenced by phase separation during polymerization, where
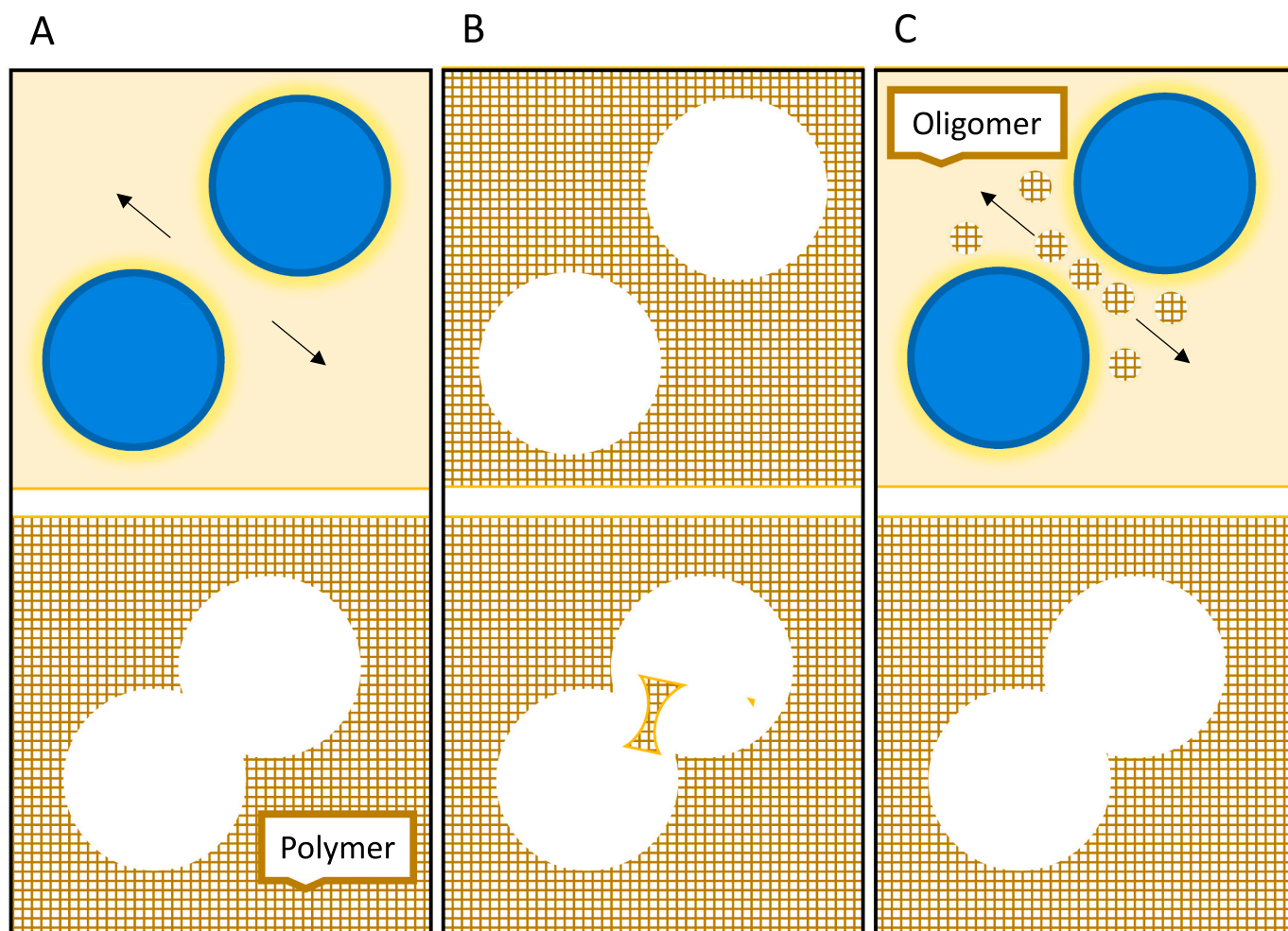
**Fig. 12.** The three proposed pore throat formation mechanisms in conventional polyHIPEs: (A) The drainage or rupture of the thin interfacial continuous film during polymerization (arrows indicates drainage from interface to Plateau border), (B) the thin polymer film between the pores of the polyHIPE is being ruptured during the post processing of the material, (C) the growing oligomer chains at the interfacial area migrate to the Plateau border where this migration induces depletion forces so that the emulsion droplets semi-coalesce during the polymerization (arrows indicate the migration of the oligomers).

surfactant-rich domains accumulate at the interfaces of neighboring droplets. These regions act as weak points that fracture during post-synthesis steps. Additionally, they highlighted that while the surfactant level is critical for forming interconnected pores, similar rupture-induced pore throats can also be observed in Pickering polyHIPEs, where nanoparticles stabilize the emulsion. Their findings emphasize that the interconnected pore structure of polyHIPEs depends significantly on both the surfactant dynamics and the mechanical stresses encountered during purification.

Recently, Foudazi highlighted an alternative viewpoint on pore throat formation due to volume contraction [29]. He states that if volume contraction during polymerization were the governing factor of pore throat formation, the locus of polymerization initiation should not affect the openness of the final product since the extent of volume contraction is the same as long as the continuous phase is the same. Because of this, he proposed an alternative mechanism; pore throat formation due to droplet/pore coalescence driven by depletion attraction (Fig. 12C). According to this mechanism, the growing oligomer chains at the interfacial area detach and migrate to the Plateau border, the edge between three adjacent water droplets. The migration of pre-polymer induces a depletion attraction to allow droplets to partially coalesce during polymerization. Pore throats are formed at the partially coalesced regions of droplets if the migration rate of detached oligomers from the interface to the Plateau border is faster than the rate of

polymerization.

Alternatively, Pawar et al. reported that Pickering emulsion droplets can be stable at a partially coalesced state if further coalescence is arrested due to particle jamming at the contact region [17](Fig. 13A). In parallel with Pawar's proposed mechanism, Durgut et al. proposed arrested coalescence as a mechanism to induce pore throats in Pickering polyHIPEs [97]. The claim was supported by the observation of a dense particle layer surrounding the pore throats as well as pore-pore junctions. The proposed mechanisms for pore throat formation in polyHIPEs are represented in Fig. 13B.

*4.2.2. Closed porous morphology of Pickering PolyHIPEs*

Pickering polyHIPEs are known for their closed porous morphology, unlike surfactant-stabilized HIPE templates [98–102]. The closed porous structure of Pickering polyHIPEs is attributed to the higher thickness and/or stability of the interfacial continuous film, which resists rupturing during polymerization or post-processing of the material, according to the commonly accepted pore throat formation mechanism. The increased stability of the interfacial film arises from the layers of particles surrounding the emulsion droplets and the formed particle network in the interfacial continuous phase [103,104]. Therefore, the stable interfacial film withstands the thinning of the interface during polymerization, preventing rupture and producing a thicker polymer interface without a significant amount of pore throats. The closest point
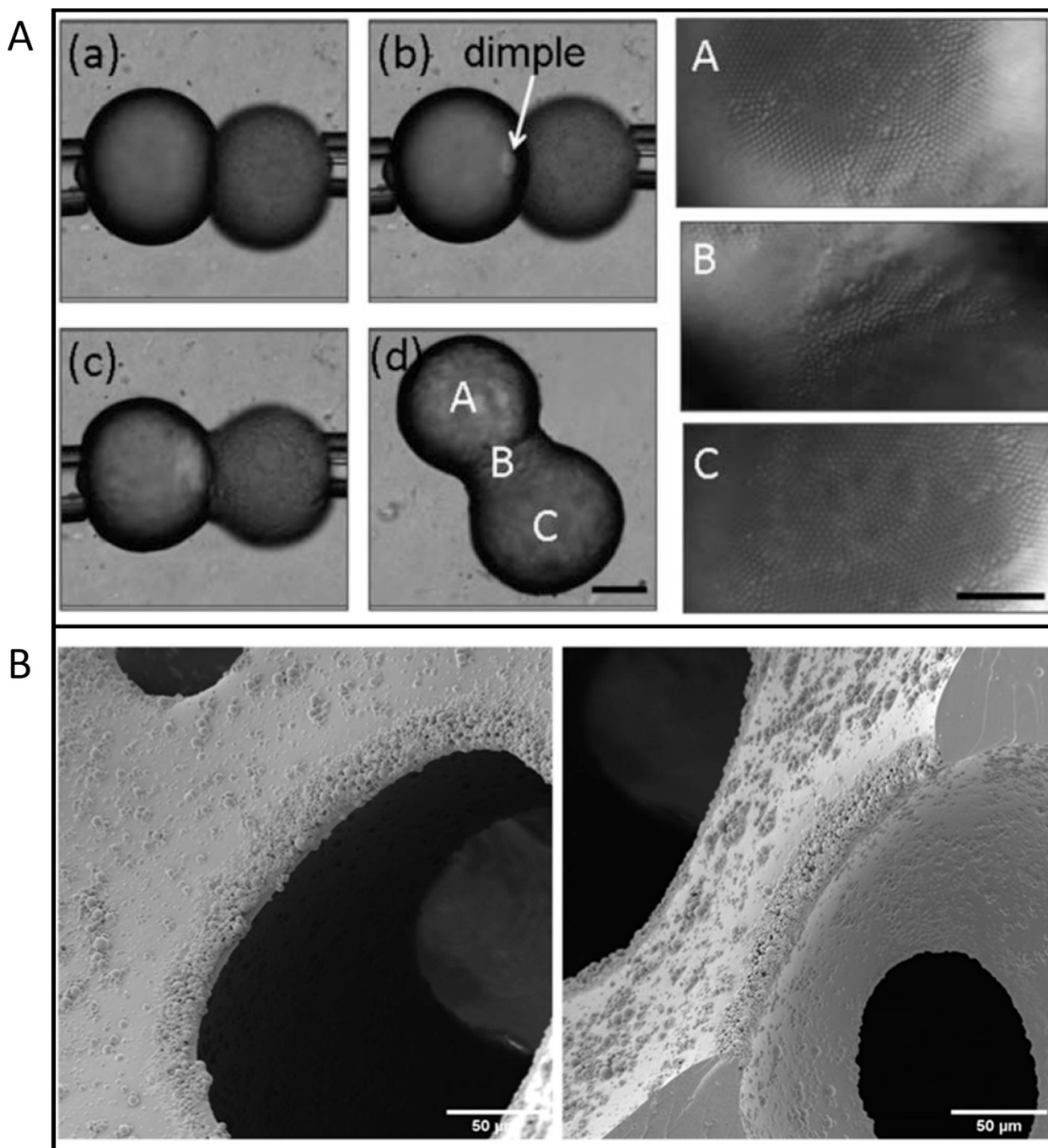
**Fig. 13.** (A) Manipulation of sparsely covered hexadecane emulsion droplets via micropipette to contact with each other and the formation of dimple at the contact region between two droplets [17]. (B) Proposed pore throat formation in Pickering PolyHIPE via arrested coalescence where the pore throats are crowded with particles indicating the dimple formation prior to polymerization [97].

between the pores manifests itself as pore throats covered with the thin polymer film, which would normally be expected to produce pore throats.

Alternatively, the closed-porous morphology in Pickering polyHIPEs is attributed to the strong adsorption of Pickering agents at the oil/water interface compared to surfactants. Droplet coalescence is hindered during polymerization due to the effective mechanical barrier formed around the emulsion droplets by colloidal particles, while small surfactant molecules can be dispersed in either of the phases when exposed to polymerization-induced forces, allowing droplets to coalesce [100]. Therefore, to introduce interconnected pores in Pickering polyHIPEs, methods to reduce interfacial stability and the thickness of the

interfacial film, as well as the induction of droplet coalescence, are utilized.

### 4.2.3. Interconnected Pickering PolyHIPEs

While Pickering polyHIPEs typically exhibit a closed-pore morphology, there are several reports demonstrating interconnected Pickering polyHIPEs. The methods presented in these reports are reviewed in this section. It is important to note that the applicability of these methods to induce pore throat formation is limited to the given experimental conditions.

*4.2.3.1. Dual emulsifiers.* The utilization of both surfactant and

colloidal particles, referred to as "dual emulsifiers," is commonly employed to introduce interconnected pores in Pickering polyHIPEs [105–109]. PolyHIPEs obtained through dual emulsification exhibit intermediate pore sizes and larger pore throat sizes than those emulsified solely by either of the emulsifiers [102,103]. Furthermore, hierarchical porous structures have been reported using this method, where the polyHIPEs exhibit both Pickering-like large and closed pores and conventional-like small and interconnected pores [99,110]. Dual emulsification is also employed to enhance HIPE stability [111,112] or to form a HIPE when the sole use of either emulsifier fails [58,113]. The amount of surfactant used in a dual emulsification system is generally less than the amount used to stabilize a HIPE as a sole emulsifier, reducing concerns associated with surfactant use. Alternatively, reactive surfactants as secondary emulsifiers can be used to minimize the possibility of surfactants leaching out from the final product [106]. On the other hand, both synergistic [54,110] and antagonistic effects [113] of dual emulsifiers on emulsion stabilization are reported (Fig. 14).

As highlighted in the previous sections (see Fig. 6), the formation of a particle network at the interface due to excess particles increases the viscosity of the interfacial film, thus enhancing interfacial film stability. The stable interfacial film resists rupturing during polymerization/post-processing, providing closed pores in polyHIPE, according to the prevailing view. Ikem et al. reported that the addition of Hypermer 2296, which cannot stabilize the HIPE at the given concentration solely, to a premade silica-stabilized HIPE disaggregated the excess particles [103]. Disaggregated particles are well dispersed in the continuous phase, resulting in reduced continuous phase viscosity [60,103]. The reduced continuous phase viscosity allows interfacial film drainage due to the sedimentation of a less concentrated emulsion, thus thinning the interfacial film where the pore throats are formed. Surfactant molecules also adsorb onto the emulsion droplets, reducing the interfacial tension between two phases [110]. Together with the reduced continuous phase viscosity and the interfacial tension, this process allows emulsion droplets to be further broken down under shear, producing smaller droplets/pores [103].

Rather than adding surfactant to the premade emulsion, dual

emulsifiers are initially dispersed in the continuous phase when the HIPE is formed. The location of the particles was investigated either by TEM [110] or fluorescent microscopy [104] and it was observed that particles are located at highly curved regions of droplets/pores—either the surface of spherical droplets/pores separated by a thick continuous phase or the droplet/pore surface neighboring the Plateau border——rather than at less curved droplet/pore surfaces where the droplets are jammed/flattened. This observation is explained by the competition between emulsifiers to localize at the oil/water interface. Surfactant molecules can rapidly localize at the oil/water interface at the less curved surface due to their small size. The pressure difference between the Plateau border and the interface due to the interfacial tension leads to the migration of unattached particles from the interface to the Plateau border while the continuous phase film is being drained. Therefore, particles locate themselves at the oil/water interface when they are not subjected to continuous film drainage. Therefore, the competition between emulsifiers to adsorb onto the oil/water interface is suggested [60,110]. On the other hand, Vilchez et al. argued for the synergistic (competitive) stabilization of dual emulsifiers mechanism and claimed an antagonistic effect on emulsion stabilization [113]. It was demonstrated that the surfactant (Hypermer 2296) preferentially adsorbs onto the particle surface (iron oxide), affecting their wettability. The addition of surfactant to the HIPE, which is stabilized by particles, causes phase separation. Enhanced emulsion stability is observed when the surfactant is combined with the particle, which is too hydrophilic to form emulsion solely. They concluded that surfactant acts as an emulsifier only after particle surfaces are saturated with the surfactant.

The dual emulsifier method is employed to obtain a hierarchical porous structure by either dissolving the surfactant in both phases [99] or only in continuous phase [54,110]. Wong et al. demonstrated that the addition of Hypermer B246SF results in the co-existence of large closed pores typical for Pickering polyHIPEs (400 μm) and small interconnected pores typical for conventional polyHIPEs (13–17 μm) (Fig. 15A-C) [113]. Interestingly, increasing the titanium concentration reduced the pore size of large pores and increased the pore size of small pores, while the surfactant concentration (0.8–8.4 % wt) did not affect
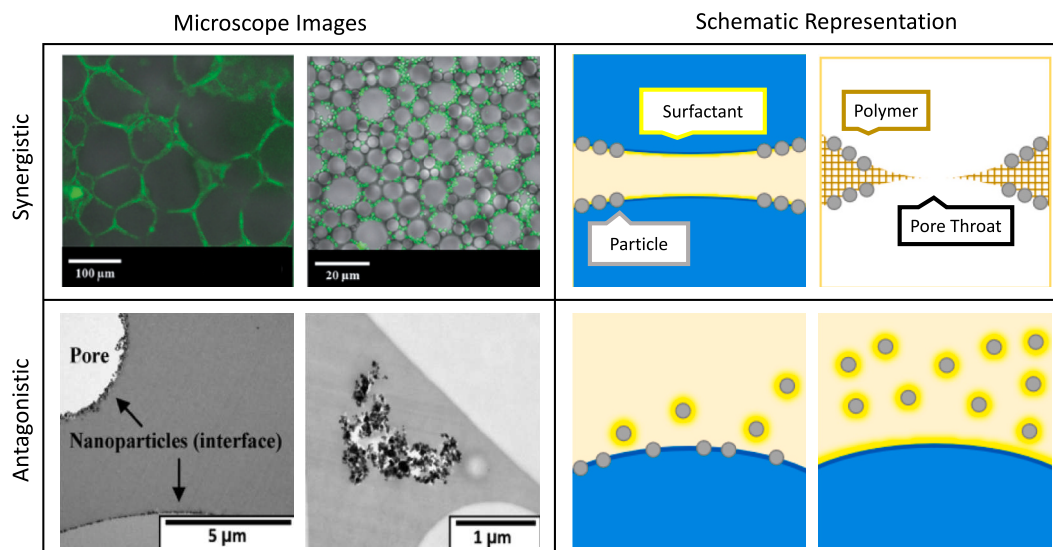


**Fig. 14.** Representation of proposed synergistic and antagonistic effect of dual emulsifier system. Synergistic effect demonstrated with confocal microscopy where the green fluorescent particles as a sole stabilizer covering the emulsion droplets (left), when the surfactant is used as co-emulsifier, particles are found at the highly curved regions of the emulsion droplets (right) (reproduced from [104] with permission from the Royal Society of Chemistry). The synergistic effect is schematically represented, where the surfactant molecules are located at the less curved region of droplets (left). These regions are susceptible to thin film rupture during polymerization, leading to the formation of pore throats (right). Alternatively, antagonistic effect of dual emulsifier system is represented in TEM images of polyHIPE. Particles as a sole HIPE stabilizer localize at the interface (left) however, when the surfactant is used, the particles are observed within the polymer in a an aggregated form (right) (Adapted with permission from [113]. Copyright 2014 American Chemical Society). The antagonistic effect is schematically represented where the surfactant is adsorbed on the particle surface first and de-attaches them from the interface (left) and surfactant function a s stabilizer only when the particle surfaces are saturated with surfactant (right). (For interpretation of the references to colour in this figure legend, the reader is referred to the web version of this article.)
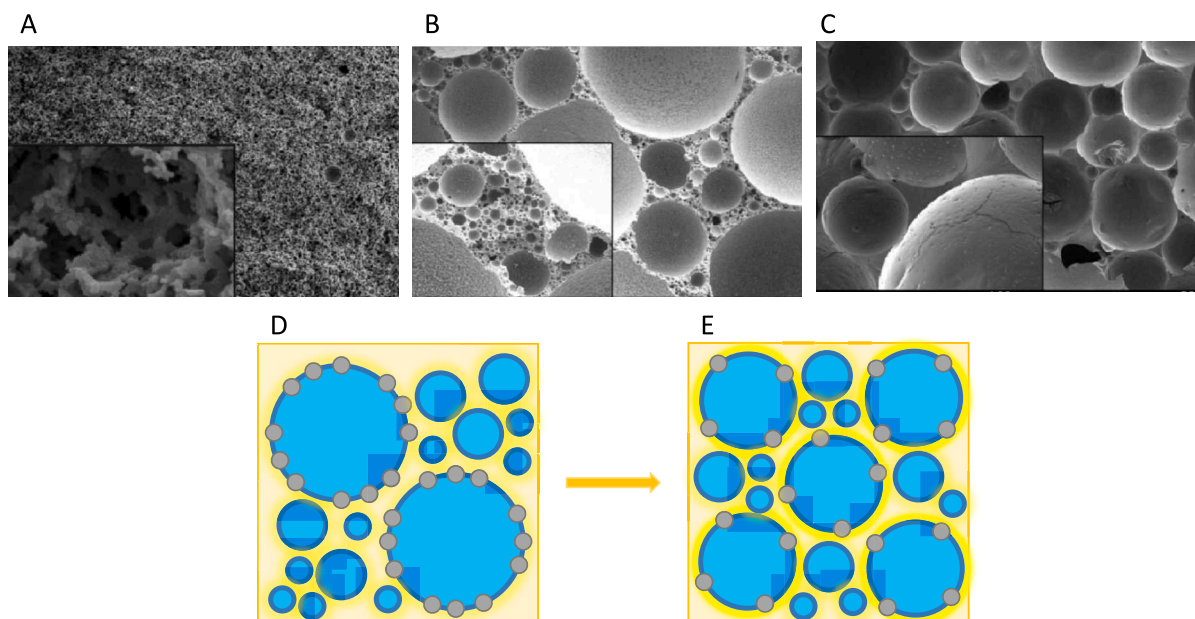
**Fig. 15.** SEM images of polyHIPEs: (A) PolyHIPEs obtained from HIPE stabilized by surfactant, (B) dual emulsifier and (C) colloidal particles. (B) The hierarchical porous structure is obtained when both surfactant and colloidal particles are used to stabilize HIPE (reproduced from [99]). Schematic representation of interplay between surfactant and colloidal particle concentration on the HIPE/polyHIPE morphology: (D) When the particle/surfactant ratio is high, large pores are mainly stabilized by colloidal particles, (E) when the particle/surfactant ratio is low, average droplet/pore size reduces.

either pore size. On the other hand, the increase in surfactant concentration was observed to increase the number of pore throats per pore. Furthermore, surfactants are also found to adsorb onto the particle surface and cause them to be dispersed in the polyHIPE polymer matrix. Further increase in surfactant concentration (17 wt%) results in the loss of the hierarchical porous structure, and the emulsion was mainly stabilized by surfactant, and the particles were dispersed in the continuous phase. A similar transition from total Pickering to conventional-like morphology as the colloidal particles to surfactant ratio is reduced is reported as well (Fig. 15D-E) [108,110,111]. Such a transition in morphology is interpreted as an antagonistic effect of dual stabilizers on pore structure by Yin et al. [108].

According to these reports, the utilization of dual emulsifier provides an interconnected porous morphology unless all the available surfactants adsorb onto the particle surface, causing particles to completely disperse within the continuous phase, leaving the system without an effective stabilizer. On the other hand, the preferential affinity of surfactant to the particles and/or droplet interface has not yet been investigated. Additionally, at which step of the emulsification the surfactant is added or in which phase the surfactant is dissolved might be another parameter affecting HIPE/polyHIPE morphology. Furthermore, the effect of depletion attraction on pore throat formation is generally overshadowed: disaggregated particles by surfactant adsorption might function as a depletant to induce pore throat formation due to depletion attraction. Alternatively, the recently hypothesized pore throat formation due to arrested coalescence can be considered; since the introduction of surfactant reduces the viscosity of the continuous phase, the reduced viscosity might facilitate the migration of particles to the necking regions of two semi-coalesced droplets to arrest droplet coalescence.

*4.2.3.2. Inducing the volume contraction during polymerization.* Since polymerization-induced volume shrinkage is one of the proposed mechanisms for pore throat formation, interconnected pores are introduced in Pickering polyHIPEs by inducing volume shrinkage either by increasing the crosslinker content [114,115] or the addition of a secondary monomer to the continuous phase that undergoes relatively

higher shrinkage during polymerization [116].

Pore throat formation is observed in vinyl ester resin-styrene (VER-St) polyHIPE when the crosslinker vinyl ester oligomer (VEO) content in the continuous phase is between 20 and 40 % (Fig. 16A) [115]. Furthermore, no pore throat formation was observed when the crosslinker content is between 0 and 10 %. Therefore, the interconnected porous structure of the Pickering polyHIPE is, in this case, attributed to increased volume contraction during polymerization. On the other hand, no pore throat formation is reported when the continuous phase consists of methyl methacrylate (MMA) rather than styrene, with 20 % crosslinker VEO. This is interesting since in another study, MMA was incorporated as a secondary monomer in the continuous phase together with the styrene to utilize the high volume shrinkage of MMA during polymerization to induce pore throat formation [116]. While the Styrene polyHIPE does not exhibit pore throats, the addition of 20 % MMA induces pore throat formation, and the gas permeability of the polyHIPE increases as the MMA content is further increased (Fig. 16B).

While inducing volume contraction is reported to obtain an interconnected porous structure in Pickering polyHIPEs, the method is not versatile. Additionally, the method necessitates a high amount of crosslinker, which might result in undesirable mechanical properties of the polyHIPE, given that high crosslinking ratios typically produce brittle polymers. On the other hand, depending on the chemistry of the crosslinker and/or secondary monomer, the localization of particles at the interface might be affected. For instance, MMA is more hydrophilic and soluble in water compared to styrene. The mixture would most probably affect the particle wettability in both phases. Therefore, pore throat formation might be much more influenced by the particle location at the interface rather than the effect of polymerization-induced volume contraction.

*4.2.3.3. Thinning the interfacial continuous phase film.* A thin interfacial, continuous phase, or polymer film between neighboring pores is the common point of the two commonly accepted pore throat formation mechanisms. Thinning the interfacial film generally results in interconnected porous Pickering polyHIPEs according to the literature. Various methods to thin the interfacial film are reviewed in this section.
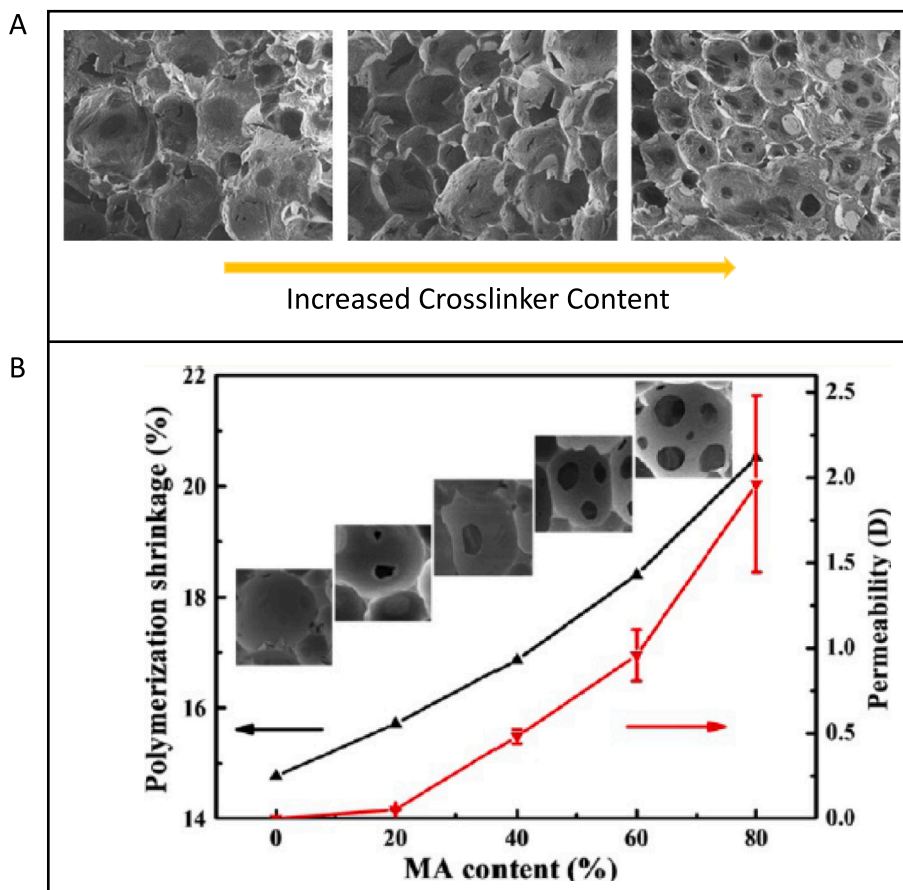
**Fig. 16.** The utilization of volume shrinkage to induce pore throat formation. (A) The increase in crosslinker content resulted in formation of pore throat. Adapted from [114]. (B) The increase in MMA content within organic phase resulted in pore throat formation due to its high volume shrinkage during polymerization. Adapted with permission from [116]. Copyright 2016 American Chemical Society.

Increasing the internal phase fraction is one straightforward way to thin the interfacial film. The increased internal phase fraction leads to shrinkage of the continuous phase both from the Plateau border and interface. It was observed that increasing the internal phase fraction leads to the formation of pore throats, whereas a lower amount of internal phase produces a closed porous morphology [114]. Additionally, increased interconnectivity is also observed for the Pickering polyHIPEs that were interconnected at lower internal phase fractions [116,117]. On the other hand, there are findings that even at a 90 % internal phase fraction, Pickering polyHIPEs exhibit a closed
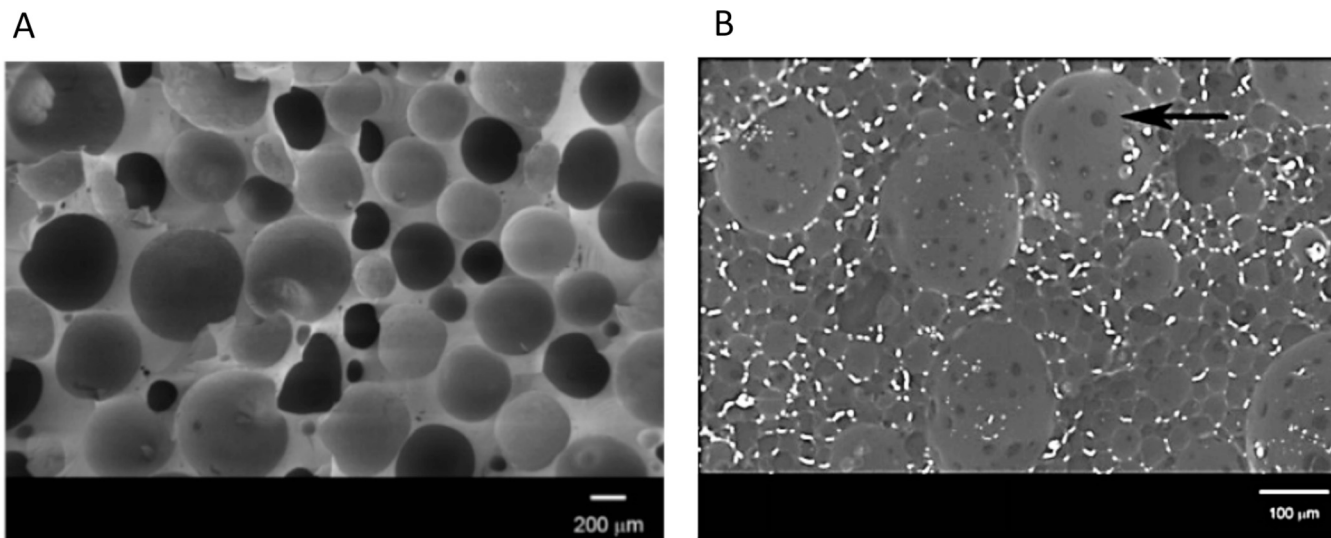


**Fig. 17.** (A) Closed cellular PolyMIPE when the CNT is the sole emulsion stabilizer, (B) open cellular PolyMIPE obtained by HIPE stabilized by CNT dispersed in the oil phase and the oxidized CNT dispersed in the water phase (black arrow indicates the pore throat). Adapted with permission from [118]. Copyright 2007 American Chemical Society.

morphology [100]. Furthermore, incorporating a higher amount of internal phase is generally impractical in Pickering polyHIPEs: the dispersion of Pickering agents in the continuous phase increases viscosity. As the internal phase is added, the viscosity is further increased, preventing the incorporation of internal phase due to inefficient mixing of the system. Menner et al. tackled this problem of increased viscosity of the continuous phase due to Pickering agent dispersion by using Pickering agents in both phases: hydrophobic carbon nanotubes (CNT) in the continuous oil phase and the hydrophilic CNT in the internal water phase to prepare polyMIPE (Fig. 17) [118].

An alternative way to thin the interface is through the extraction of the continuous phase from the interface by particles or the structures formed by particles. It was observed that non-crosslinked styrene particles as a stabilizer result in interconnected Pickering polyHIPEs, while crosslinked styrene does not [119]. The pore throat formation was attributed to the swelling of non-crosslinked styrene particles by the continuous phase at the interface, resulting in a thinned interfacial continuous film. Further increase in interconnectivity is achieved by etching the non-crosslinked particles located at the pore wall with THF treatment. On the other hand, Durgut et al. reported that non-crosslinked isobornyl acrylate particles were subjected to dissolution when suspended in the continuous phase and the resultant polyHIPE exhibit surfactant-stabilized HIPE template grade small but closed porous structure [120]. While the cross-linked IBOA particles yielded interconnected polyHIPEs.

Alternatively, Zheng et al. reported interesting differences between octadecyltrimethoxysilane (ODS) modified silica particle-stabilized polyHIPEs when the particles are dispersed in either the water or the oil phase [121]. Only when the particles were dispersed in the internal water phase, did the Pickering polyHIPE exhibit an interconnected structure. It was observed that particles effectively disperse in the continuous phase but form aggregates when dispersed in the internal phase. These aggregates form micelle-like structures, where the shell is hydrophilic but the core is hydrophobic. Therefore, the interfacial continuous phase diffuses into the micelle-like silica aggregate, resulting in a thinned interfacial film and throat formation.

*4.2.3.4. The effect of particles: Localization and interaction.* Pickering agents, functioning as an effective barrier around the emulsion droplets and their strong adsorption at the interface, are considered the main reasons for obtaining a closed porous morphology in Pickering polyHIPEs. From this perspective, methods to tune the particle localization at the oil/water interface or re-localization/migration of Pickering agents from the interface during polymerization can be exploited to obtain pore throat formation. Therefore, papers reporting close to open porous morphology due to particle localization are reviewed in this section.

Pickering agents are generally subjected to surface modifications to tune their wettability to obtain a stable HIPE. The wettability affects the localization of particles at the interface. Several papers investigate the effect of surface modification of Pickering agents on the morphology of Pickering polyHIPEs. For example, in graphene oxide (GO) nanosheet-stabilized HIPEs, the degree of CTAB modification on graphene oxide nanosheets is reported to affect the openness of the acrylic acid Pickering polyHIPE [57]. Non-modified GO nanosheets produce closed-cell polyHIPEs, while an increase in the degree of cetyltrimethylammonium bromide (CTAB) modification introduces pore throats. Decomposed CTAB from the nanosheet surface might be a factor affecting the interconnectivity, but the study demonstrates that a further increase in CTAB modification reduced the interconnectivity. While the author attributed the pore throat formation to the geometry and the atomic scale thickness of the nanosheets (thinner than common Pickering agents), CTAB-modified GO nanosheets were also used in another study to prepare styrene polyHIPEs that exhibit a closed porous morphology [122]. Additionally, pore throats were rarely observed.

This was attributed to the decomposed CTAB from the nanosheet surface. Considering the difference in the hydrophobicity of the organic phase and the sensitivity of the Pickering polyHIPE openness to the degree of surface modification, the pore throat formation might be more relevant to the localization of Pickering agents rather than atomic scale thickness of the stabilizer. As mentioned in the previous section, the degree of ODS modification of silica particles affected the openness of styrene Pickering polyHIPE when dispersed in the internal water phase initially. While the mechanism is attributed to the monomer extraction due to silica aggregates, the reduced amount of ODS modification resulted in a closed porous morphology even if it is dispersed in the internal phase [121].

An interconnected porous structure was observed in melamine-formaldehyde (MF) Pickering polyHIPE where lignin particles were the stabilizer. Pore throats were only formed if the concentration of pre-MF in the continuous water phase is above 25 %. The mechanism of the pore throat formation was attributed to the reaction between the lignin particles and pre-MF, which provides the force to draw particles from o/w interface to Plateau border [100]. Consequently, the pore throats are formed either due to droplet/pore coalescence or a sufficient thinning the interface to rupture since the barrier separating two neighboring droplets is removed during polymerization. The closed to open porous morphology was also observed in MF Pickering polyHIPEs where the stabilizer was dialdehyde cellulose-aniline with various aldehyde to aniline molar ratios [123]. Pore throats were observed when the aldehyde to aniline molar ratio was 20:1, and a closed porous morphology was obtained at reduced aldehyde to aniline molar ratios. On the other hand, the pore throat formation was attributed to obtained smaller pore size, rather than monomer-particle interaction or the wettability of Pickering agents. Alternatively, sulfonated polystyrene particles in tetrahydrofuran solution were used as an emulsion stabilizer to obtain either styrene or butyl acrylate polyHIPEs [124]. While the styrene polyHIPEs exhibit a closed porous morphology, an interconnected porous structure was obtained in butyl acrylate polyHIPEs.

*4.2.3.5. Other.* Interconnected Pickering polyHIPEs were reported when non-crosslinked Styrene-Methyl Methacrylate-Acrylic Acid (St-MMA-AA) particles were used as a stabilizer in the study of Hua et al. [125]. In this system, there was no monomer to polymerize; and the particles functioned as a stabilizer as well as building blocks forming the material's skeleton. Particles were dispersed in the internal phase, and a water-in-toluene emulsion (anti-Finkle, the dispersion of stabilizer in the internal phase) was obtained. Since toluene dissolves the non-crosslinked particles, the dissolved polymer formed the skeleton, and yet-to-be-dissolved particles functioned as a stabilizer. The interconnectivity of the samples was observed to be strictly dependent on the standing time of the emulsion before solidification. As the standing time increased, more particles were being dissolved, which reduces the interconnectivity of the HIPE template (Fig. 1.18 A). In parallel, chitin nanofibrils were used as a stabilizer as well as the skeletal material of HIPE templates from a cyclohexane-in-water HIPE. Subsequent removal of both the continuous and the internal phase from the emulsion left behind an interconnected chitin HIPE template [126]. In this system, nanofibrils were not subjected to dissolution. Polyurethane/vinyl ester oligomer nanoparticles were utilized in a similar fashion; to stabilize cyclohexane-in-water HIPE and to form the skeleton. On the other hand, the polyHIPE did not exhibit pore throats but an open morphology with aligned pore walls due to the unidirectional freezing of the HIPE and subsequent lyophilization [127]. It was reported that the increased particle concentration negatively affects the channel formation through the pores because of preventing the ice crystal formation during unidirectional freezing (Fig. 18B).
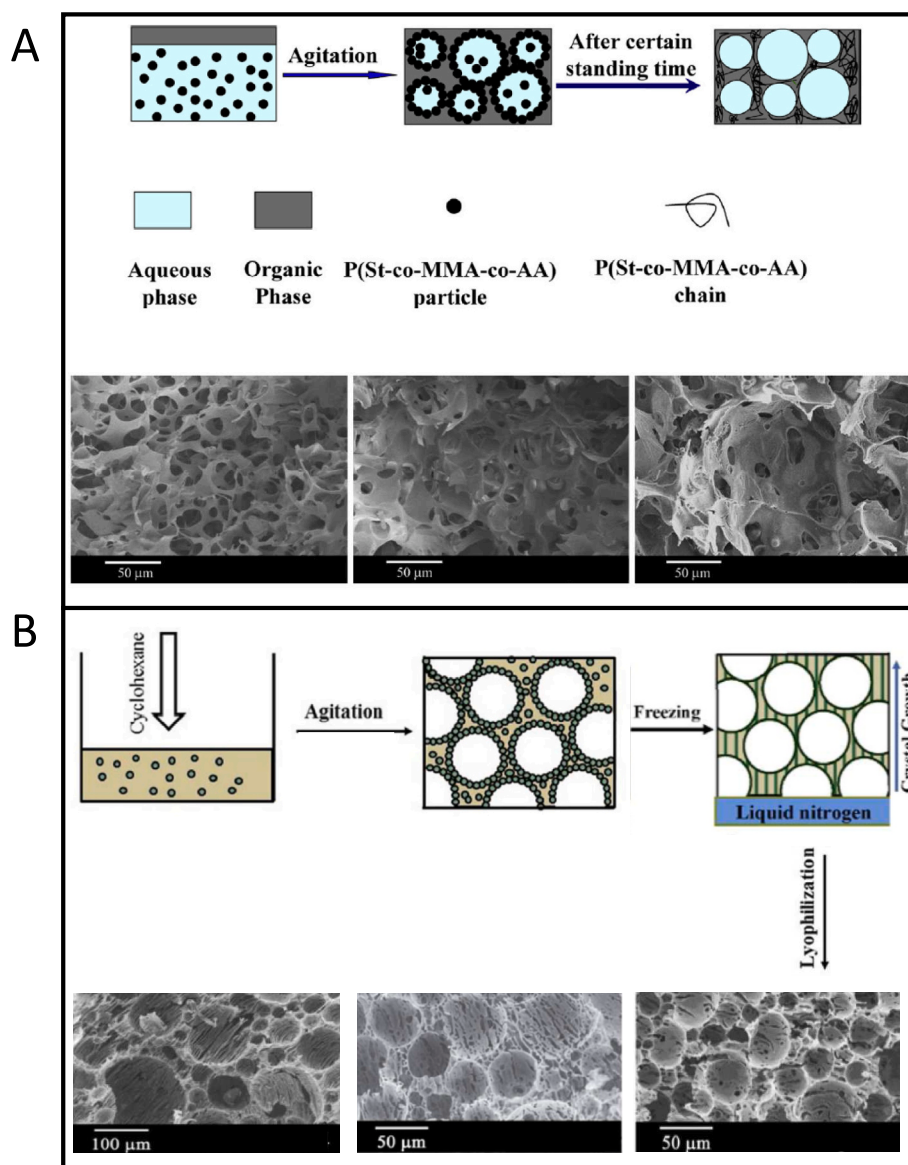
**Fig. 18.** (A) The schematic representation of the formation of anti-Finkle emulsion where the stabilizing particles are dispersed in the internal phase initially. As the particles interact with the continuous phase where they are soluble, particles disintegrate into polymeric chain and forming the material skeleton. The SEM images of the anti-Finkle emulsion templates demonstrating the loss of interconnectivity of the HIPE template as the standing time of the HIPE increase; 0, 24 and 48 h after preparation from left to right (reproduced from [125]). (B) A schematic representation of the channel formation in Pickering emulsion template by unidirectional freezing. The SEM images of the obtained templates and the effect of the increasing particles concentration (15, 25 and 30 %wt particle concentration from left to right) on the channel formation. Adapted with permission from [127]. Copyright 2016 American Chemical Society.

### 4.3. The morphological characterization of PolyHIPEs

#### 4.3.1. Porosity

The internal phase of the HIPE represents itself as pores in poly-HIPEs. Therefore, the volume fraction of HIPE's internal phase is equal to the total pore volume of the polyHIPE, theoretically. However, this value may vary in practice. HIPE can experience destabilization after being prepared or during polymerization, especially when subjected to elevated temperatures for a long time during thermal polymerization. Depending on the material used, the monomer-to-polymer conversion during polymerization may result in shrinkage in polyHIPE. Alternatively, the porous structure of the polyHIPE can collapse during post-processing due to capillary stress induced during washing/drying steps.

The cost-effective method to deduce the porosity of the polyHIPE is using the difference between the skeletal ($\rho_{sd}$) and bulk density ($\rho_c$) of the polyHIPE [128,129]. Assuming that the samples are in known

geometrical shape, both $\rho_{sd}$ and $\rho_c$ can be obtained from simple mass and volume measurements of the bulk polymer and the polyHIPE, respectively. $d_s$ can be deduced from obtaining the volume of the polyHIPE via the graduated cylinder method (aka liquid displacement method) as well [130,131]. Alternatively, $\rho_{sd}$ and $\rho_c$ can be measured via dedicated devices; pycnometer and envelope density analyzer, respectively [78].

Porosity as well as the specific surface area can be measured through mercury porosimeter [74,132,133] as well as $N_2$ adsorption/desorption test. The isotherms obtained from $N_2$ adsorption/desorption are analyzed with the Barret-Joyner-Halenda method [74]. The isotherms can be further used to calculate the specific surface area of the polyHIPE when analyzed with the Brunauer-Emmett-Teller (BET) method [134,135].

Except for the utilization of density difference between $\rho_{sd}$ and $\rho_c$, the methods necessitate access to the pores, such as $N_2$, mercury, etc. Therefore, these methods are only reliable if the polyHIPE exhibits an

open porous structure. To evaluate the fraction of dead-end pores, Mravljak et al. calculated static porosity by measuring both wet and dry mass as well as wet volume of the polyHIPE and measured the flow through the porosity pulse experiment measuring conductivity [70]. The difference between the static and flow-through porosity represents the volume fraction of the dead-end pores.

### 4.3.2. Cellular structure

The cellular structure of a polyHIPE includes pore size, shape, and distribution; pore throat size and distribution; as well as strut thickness and aspect ratio. Therefore, the evaluation of the cellular structure is mainly dependent on imaging techniques and further analysis through software.

Assuming that the effect of polymerization-induced forces is minimal, pore size and distribution can be deduced from the evaluation of HIPE droplets by acquiring micrographs through light microscopy or methods like dynamic light scattering or laser diffraction. It has been previously demonstrated that polyHIPE itself can be imaged through light microscopy but necessitates labor-intensive sample preparation [130]. To directly image the polyHIPE, scanning electron microscopy (SEM) is the commonly used method. The micrographs acquired through SEM can be used to analyze all the microfeatures of the polyHIPE. Since the samples are sectioned, the imaged pores do not represent the actual sizes of the pores (Fig. 19). Therefore, a statistical correction factor is applied to the measured pore sizes, assuming that all the pores are sectioned from R/2 distance from the middle of the pores. The statistical correction factor is found to be $2/\sqrt{3}$ [74], or $4/\pi$ [70] if the equation is integrated through the actual radius of the pore. Recently, Pore D$^2$, an automated tool for measuring pore sizes from SEM images, was introduced to simplify and enhance the accuracy of pore analysis [136]. Additionally, X-Ray microcomputed tomography (μCT) is used to evaluate the polyHIPE in 3D after reconstructing the collected 2D images (Fig. 20) [137,138].

The pore throat size and distribution are crucial for evaluating the degree of interconnectivity and openness of the pores. SEM micrographs can be used to deduce the average pore throat size and distribution. Since the pore throats are distributed on the hemispherical pores in the micrographs, their size is affected by the angle at which they are viewed [129]. Therefore, the pore throats are considered as ellipsoids, and the long axis of the ellipsoid is used as the pore throat diameter. Counting the number of pore throats per pore, and thus the overall open surface on the pore, is affected by the uneven sectioning of the pores as well. Therefore, the number of pore throats counted on SEM micrographs is multiplied by 4 [70].

Two terms are generally used to report the pore throat/pore relationship of polyHIPEs; the degree of interconnectivity [130,139] which is the ratio between the average pore throat size to the average pore size, and the degree of openness [140] which is the ratio between the overall pore throat area to the pore surface area. Alternatively, the permeability of the polyHIPE provides data to compare the openness of the polyHIPEs



**Fig. 19.** Schematic representation of uneven sectioning of polyHIPEs. R and r represents the actual and the sectioned radius of the pores.

[99]. Instead of using SEM, mercury porosimetry provides the size and distribution of the pore throats of polyHIPEs by gathering the accessed volume at increased pressure. The higher the pressure, the smaller the pore throats that have been accessed. Normally, mercury porosimetry is a method to acquire the porosity/pore size of porous samples. However, in polyHIPEs, it provides pore throat size data rather than pore size since the mercury flows through pore throats [74].

## 5. Mechanical properties of pickering polyHIPEs

PolyHIPEs, being highly porous, are known for their reduced mechanical properties compared to their non-porous counterpart. Although the mechanical properties of a material depends on the application necessities, the mechanically weak materials can be an issue when in industrial usage. Therefore, understanding the governing parameters affecting the mechanical properties of these highly porous materials and tuning their mechanical properties are crucial research areas. The intrinsic mechanical properties of the materials forming the skeleton of the polyHIPE, such as isobornyl acrylate polyHIPE and 2-ethylhexyl acrylate polyHIPE exhibiting 50 and 1 MPa Young's modulus, respectively, can be tuned by adjusting the composition of constituent monomers [141]. Pore volume is another determinant of polyHIPE mechanical properties, directly related to foam density, where an increase in pore volume leads to a decrease in mechanical properties [141–146]. Since the higher porosity is the integral part of polyHIPEs, decreasing the total pore volume is not a feasible method to produce polyHIPE with increased mechanical properties. Therefore, the effect of pore organization, distribution, and HIPE stabilizers (surfactants or colloidal particles) on the mechanical properties of polyHIPEs is reviewed in this section.

Both pore size and distribution influence the mechanical properties, with larger average pore sizes increasing properties due to thicker polymeric struts [147]. Additionally, the hierarchical organization of pores were reported to increase the mechanical properties of polyHIPEs [148]. Wong et al. demonstrated that the polyHIPE with large-closed and small-open hierarchical pore organization exhibit improved Young's modulus (~24 MPa) compared to both large-closed (~12 MPa) and small-open (~1 MPa) porous polyHIPEs [99]. Additionally, interconnectivity of the pores is another morphological feature affecting the mechanical properties. The structural integrity of the pores are negatively affected by the openness of the pores, resulting in the decreased mechanical properties [37,74].

Adjusting the stabilization mechanism, whether using a surfactant or Pickering agent, is considered another approach to tune the mechanical properties of polyHIPEs. However, changing the type of stabilizer is accompanied by morphological differences in polyHIPE. Therefore, understanding the direct effect of stabilizer type on mechanical properties can be challenging. Nevertheless, the type of stabilizer can influence mechanical properties in a more complex manner rather than by simple tuning pore size and/or interconnectivity. For instance, Kovacic et al. investigated the effect of surfactant (Pluronic L-121) loading, ranging from 0 % to 10 %, on polyHIPE mechanical properties and observed a significant decrease in Young's modulus when surfactant loading exceeded 5 % [83]. The observed change in Young's modulus did not correlate simply with the decreasing pore and pore throat size. The study claimed that the remaining surfactant on the polymer wall, which cannot be purified from the material, acts as a plasticizer, negatively affecting mechanical properties. Further increases in surfactant lead to the production of monomer-filled micelles, which are polymerized within the monomer and washed out of the material skeleton, resulting in a further reduction of foam density.

Colloidal particles, when used as a filler, have demonstrated the ability to increase the mechanical properties, including Young's modulus and crush strength, of polyHIPEs when covalently bound to the polymer [144,145]. Additionally, colloidal particles, when employed as a stabilizer, have shown similar increase in mechanical properties
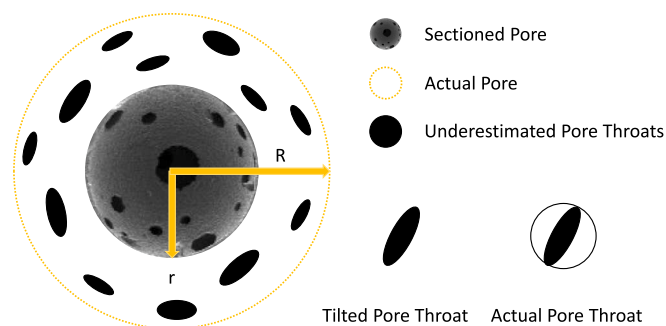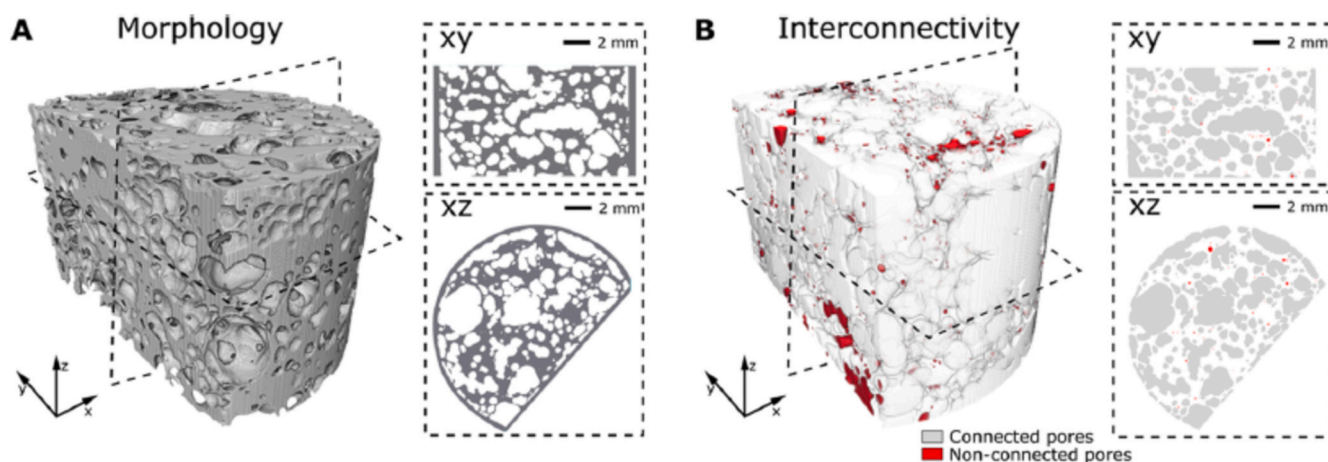
**Fig. 20.** The reconstructed 3D image and the 2D images from two different planes of a polyHIPE obtained from μCT (reproduced from [137]).

[149,150]. The impact of colloidal particles on the mechanical properties of polyHIPEs is generally attributed to their distribution on the pore surface. Increased mechanical properties are observed when pore surfaces are evenly covered with particles, creating an efficient network for stress transfer from the polymer to the particles [88]. However, an increase in particle concentration beyond the optimum loading concentration leads to a decrease in mechanical properties due to particle aggregation, which acts as stress concentration points [150,151].

## 6. Applications of Pickering PolyHIPEs

Due to their highly interconnected porous structure and consequently large surface area, conventional polyHIPEs find applications in various fields such as catalyst support, tissue engineering scaffolds, and adsorbents. Pickering polyHIPEs can be considered a more environmentally friendly alternative to conventional polyHIPEs by either eliminating or reducing the usage of surfactants, leading to reduced production costs. From a morphological perspective, the intrinsic large pores and rough pore surfaces of Pickering polyHIPEs can offer improved performance depending on the application, despite some contradictory reports. The enhanced mechanical properties of Pickering polyHIPEs can be particularly beneficial for applications that require durable materials. Importantly, the integration of particles on the pore walls adds intrinsic functionality to Pickering polyHIPEs. In this section, we will review reports demonstrating the applications of Pickering polyHIPEs.

### 6.1. Catalyst support

One of the most common applications of Pickering polyHIPEs is their utilization as a catalyst support. Catalytic activity can be achieved by decorating the pore walls with functional colloidal particles. Alternatively, colloidal particles can be subsequently used to tether functional nanoparticles to the polyHIPE surface. For example, Yi et al. used synthesized tadpole-like single-chain polymer Janus nanoparticles, where the tail and the head are composed of polyMMA and poly(4-vinylpyridine), respectively [117]. The nanoparticles were used as the sole stabilizer to produce open-porous St/DVB polyHIPE. Due to the strong interaction between the poly(4-vinylpyridine) head of the stabilizer and metal nanoparticles, the polyHIPE was successfully loaded with palladium nanoparticles and further used as a catalyst for the Suzuki-Miyaura carbon-carbon coupling reaction.

$TiO_2$ is one of the most commonly used Pickering agents. Due to its photocatalytic activity, Pickering emulsion templates stabilized by $TiO_2$ are mainly used as photocatalyst support. Li et al. produced $TiO_2$-decorated polyHIPEs by templating an o/w HIPE stabilized by $TiO_2$ and poly(isopropylacrylamide-*co*-methyl methacrylate) microgels [152]. After sintering the material, the photocatalytic activity of the template was evaluated by the photodegradation of Rhodamine B and reported that the template exhibits better performance compared to commercially available P25 samples. Zhu et al. used $TiO_2$ to produce acrylamide Pickering polyHIPE beads and demonstrated its photocatalytic activity by degrading methyl orange (MO) [153]. While the polymer beads were not as effective as pure $TiO_2$ at the beginning of the test, after 2.5 h of treatment, 99.4 % of MO was found to be degraded, similar to pure $TiO_2$ nanoparticles. Additionally, there was no reduction in the photocatalytic performance of the porous beads until 9 cycles of usage. On the other hand, there was no significant difference in photocatalytic performance between the porous beads prepared with a different amount of $TiO_2$ particles due to the limited UV penetration into the beads to excite remaining $TiO_2$ particles within the polymer matrix rather than a pore surface. On the other hand, Yuce et al. demonstrated that the loading of $TiO_2$ increases the photocatalytic degradation of 4-nitrophenol of the surface-modified $TiO_2$ particle stabilized emulsion template of poly-dicyclopentadiene [154].

In addition to $TiO_2$, various functional colloidal particles decorated Pickering polyHIPEs have been used for various catalytic activities. Lee et al. used silver-incorporated melamine-based microporous organic polymers (m-MOP/Ag) as the sole stabilizer to obtain a hydrophilic and open-porous acrylamide polyHIPE [155]. The resultant monolith was utilized as a heterogeneous catalyst to reduce 4-nitrophenol in an aqueous medium. It is reported that the rate constant of the reaction is 7 times faster with the polyHIPE compared to the bulk m-MOP/Ag composite, suggesting that the catalytic sites are accessible due to the interconnected porous nature of the polyHIPE. Sun et al. prepared a zeolitic imidazolate framework (ZIF-8) porous HIPE template by utilizing ZIF-8 as a stabilizer and the material to form the skeleton by bonding ZIF-8 nanoparticles within the continuous phase [156]. The ZIF-8 monolith was used as a catalyst for the flow-through Knoevenagel reaction, and it was observed that the monolith reacts with benzaldehyde with a conversion rate of 100 %. Gao et al. produced an open-porous solid acid by sulphonation of Pickering Poly(DVB-sodium p-styrene sulfonate) and demonstrated its catalytic activity by converting cellulose into 5-hydroxymethylfurfural [157]. Pan et al. further improved the system by increasing the surface area of the polyHIPE through hyper-crosslinking and demonstrated its superior catalytic activity [101]. While the obtained polyHIPE lacked pore throats, it exhibited mesopores due to hypercrosslinking.

### 6.2. Sorbent

Due to their high porosity and high surface area, polyHIPEs are used

as sorbent. The utilization of Pickering emulsion templates as an adsorbent is highlighted in an excellent review by Zhu et al. [158]. In the case of Pickering polyHIPEs, large porous structure is beneficial since it allows the efficient mass transport. Since polyHIPEs as a sorbent material necessitates the interconnected porous structure, they are generally prepared from surfactant/particle dual emulsified HIPEs. Additional selectivity toward specific target such as pollutants or oil/water and metal ions can be achieved due to functional particles decorating the pore walls. For example, Yang et al. demonstrated the $Cu^{2+}$ adsorption capacity of interconnected lignin stabilized melamine formaldehyde HIPE template from $CuSO_4$ solution up to 73 mg g$^{-1}$ [100]. Similarly, acrylamide Pickering polyHIPE hydrogels were demonstrated to adsorb $Cu^{2+}$ up to 280 mg g$^{-1}$, thanks to ionic functional groups on the material [57].

The efficacy of Pickering polyHIPEs as a sorbent material in $CO_2$ capture were demonstrated in several reports. Metal-organic-frameworks (MOFs) are commonly used functional stabilizer in Pickering polyHIPEs for $CO_2$ capture due their unsaturated metal centres which can interact with $CO_2$ [159,160]. Alternatively, He et al. prepared 4-vinylbenzyl chloride polyHIPEs and used them as $CO_2$ adsorbent after the introduction of quaternary ammonium chloride groups to polyHIPE [107]. It was observed that surfactant/Pickering dual emulsified emulsion templates exhibit better $CO_2$ capture compared to both solely surfactant stabilized emulsion templates and commercially available Excillion membranes. The better performance of surfactant/Pickering polyHIPE system is attributed to the larger pore size of the polyHIPE. The larger pore size of the polyHIPE allows efficient mass transfer which facilitates air transport through the material and efficient quaternization/ion exchange, increasing the $OH^-$ groups on the polymer. Wang et al. utilized polyethyleneimine enveloped $TiO_2$ nanoparticles and Span 80 as a stabilizer to produce a St/DVB Pickering polyHIPE for $CO_2$ capture [150]. The $CO_2$ adsorption capacity of Pickering polyHIPE was approximately 15 % higher than that of polyHIPE prepared by Span 80 only. The superior performance of Pickering polyHIPE is attributed to the increased surface area of amine groups on the pore surface due to embedded $TiO_2$ particles which where enveloped with PEI.

Sulfonated polystyrene was used as a stabilizer to obtain butyl acrylate Pickering polyHIPE for oil spill recovery application [161]. Various fuels/solvent-water mixture was used as a spilled oil model and it was observed that absorption capacity of the polyHIPE ranging between 11.2 and 37.5 g g$^{-1}$. Similarly, Azhar et al used iron oxide nanoparticles together with a fluorinated surfactant to obtain hexafluorobutyl Pickering polyHIPEs with magnetic properties [111]. Pickering polyHIPEs demonstrated to absorb 14 g g$^{-1}$ and 10.25 mg g$^{-1}$ of DCM and methylene blue, respectively. The oil adsorption capacity of Pickering polyHIPE was double the capacity of conventionally prepared polyHIPE. The magnetic property of the polyHIPE is also beneficial to guide the material to collect oil simply by magnet. Ehtyl cellulose (EC) nanoparticles were HIPE templated and demonstrated it is application to oil/water separation [40]. A droplet of n-decane-in-water emulsion was separated upon contact with the EC porous material due to adsorption of n-decane by EC. Similarly, the ZIF-8 Pickering polyHIPE was used as oil adsorbent and exhibited high absorption rate, reaching the equilibrium as fast as in 5 s, compared to bulk ZIF-8 [156]. Abebe et al. used methylcellulose/tannic acid stabilized alginate/polyacrylic acid Pickering polyHIPE as an amphiphilic adsorbent, for the removal of methylene blue and quinoline from aqueous and non-aqueous environment, respectively [162]. Both the skeleton of the polyHIPE and the particles on the pore walls were responsible for methylene blue removal from an aqueous solution, while only the particles contribute the removal of quinine from non-aqueous solution since the polyHIPE material itself was hydrophilic. $Al_2O_3$ stabilized acrylic acid HIPE template was used as superabsorbent [114]. The obtained polyHIPE exhibit superabsorbent ability, absorbing above 40 g g$^{-1}$ water and saline solutions. The crosslinking density of the material is shown to affect the absorption capacity, since a lightly crosslinked polymer wall can absorb water more

efficiently than highly crosslinked counterparts. $Fe_3O_4$ nanoparticle stabilized acrylamide HIPE templates used as water absorbent and demonstrated its efficiency of separating water phase from a surfactant stabilized emulsion [163].

### 6.3. Encapsulation

The closed pores of Pickering polyHIPEs are used to encapsulate materials for further applications. Depending on the application, closed cellular morphology of conventional Pickering polyHIPEs can be advantageous if the release of the encapsulated material is not intended [164,165]. Alternatively, open-cellular Pickering polyHIPEs are generally preferred if the encapsulated materials, such as drugs, are expected to be released [166].

Elastomer-filled hydrophilic polyHIPEs were prepared by templating either surfactant or nanoparticle-stabilized HIPE, and their water adsorption capacities were compared [164]. In the synthesis, the continuous phase consisted of the hydrophilic monomer, sulfonated styrene, and the internal phase consisted of 2-ethylhexyl acrylate. The obtained polyHIPE pores were filled with crosslinked EHA elastomer, regardless of the stabilizer used. Interestingly, a significant difference in water absorption capacity, up to three times, between the produced polyHIPEs was observed. The inferior water absorption capacity of conventional polyHIPEs was attributed to the copolymerization of SS in the continuous phase and the EHA in the internal phase. The incorporation of hydrophobic EHA into the macromolecular structure reduced the hydrophilic character of the polyHIPE. Such copolymerization was not observed in Pickering polyHIPEs due to the efficient barrier effect of particles preventing the interaction of two phases with each other. Similarly, elastomer-filled Pickering polyHIPEs are demonstrated to exhibit shape memory foams [165]. The polyHIPE skeleton is composed of semi-crystalline, long side-chained polyacrylates, and the nanoparticles are used as both emulsion stabilizer and crosslinker. Interestingly, the material demonstrated to exhibit dual lock-in shape memory; when the polyHIPE is subjected to water above the melting temperature of the polymer composing the skeleton, the crystalline structure melts, the hydrogel structure plasticizes and allows the elastomer to recover the original shape of the material. When the polyHIPE is synthesized with the surfactant and conventional crosslinker, copolymerization takes place between the monomers within both phases, and this copolymerization reduces the side chain mobility, therefore, reducing the shape recovery behaviour of the material.

Pickering polyHIPEs have recently been employed for encapsulating phase change materials (PCMs) for thermal energy storage. Both organic PCMs, such as octadecane [167,168] and dodecanol [169] and inorganic PCMs like calcium chloride hexahydrate [170] were successfully encapsulated within the pores of Pickering polyHIPEs, serving as the internal phase during HIPE preparation. The intrinsic closed-cellular morphology of Pickering polyHIPEs, combined with interfacial initiation of polymerization, facilitates efficient PCM encapsulation within the pores while minimizing PCM leakage. Despite the inherent low thermal conductivity of polymers, a crucial property in thermal energy storage and release, enhanced thermal conductivity is achieved through the incorporation of particles with good thermal conductivity. Lu et al. not only demonstrated the heat storage capacity of PCM-encapsulated polyHIPE but also its light-to-heat conversion efficacy. They achieved this by using carboxylated carbon nanotubes (CNT) as a HIPE stabilizer to decorate the pores (Fig. 21A) [168]. Conversely, due to the low thermal conductivity of polymers, a cellulose-based Pickering polyHIPE was demonstrated for thermal insulation, leveraging its intrinsic low thermal conductivity, closed porous morphology, and low density (Fig. 21B) [171].

PolyHIPEs can serve as effective carriers for drug encapsulation, producing bioactive scaffolds for tissue engineering applications. Hu et al. loaded Ibuprofen, an anti-inflammatory drug, within Pickering PLGA emulsion templates obtained by solvent evaporation [88]. The
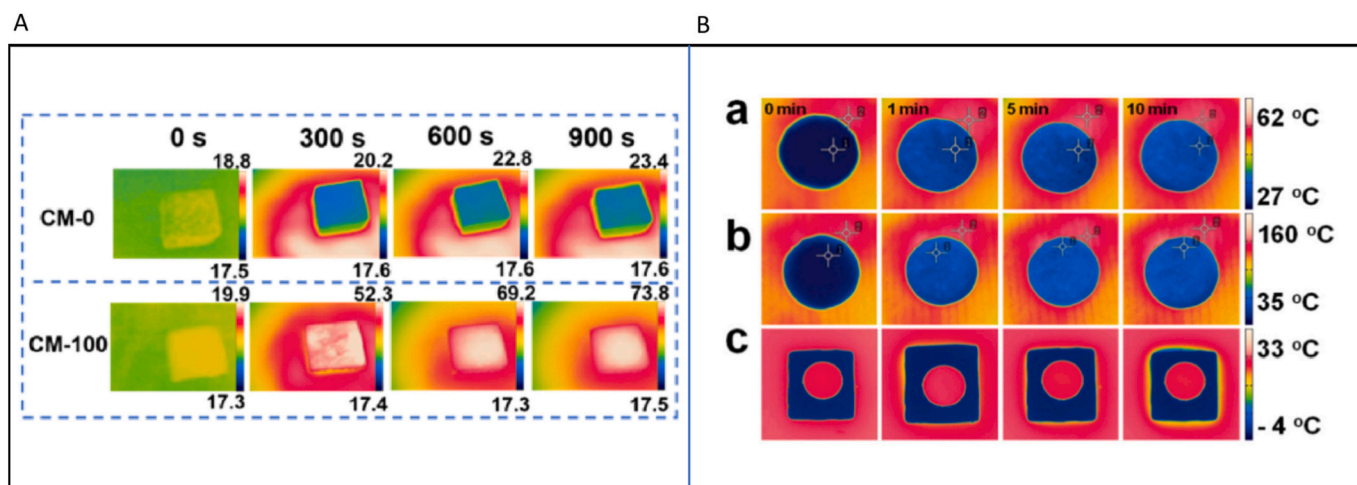
**Fig. 21.** (A) The infrared images of polyHIPE (CM-0) and carboxylated CNT incorporated Pickering polyHIPE (CM-100) captured at different times under light irradiation, demonstrating to light-to-heat conversion of CNT incorporated Pickering polyHIPE. Adapted with permission from [168]. Copyright 2022 American Chemical Society. (B) The infrared images of polyHIPE demonstrating their low thermal conductivity: PolyHIPE on a hot plate (a, b) and on ice (c) (reproduced from [171]).

scaffold exhibited an initial burst release, with approximately 55 % of the drug released within 24 h, followed by sustained slow release, reaching around 65 % of drug release in 196 h. The fast and slow drug release profiles were attributed to the initial release from the outer surface of the scaffold and the increased diffusion path from the inner side of the scaffold, respectively. Similarly, Artemisia argyi oil (AAO) was loaded into an acrylamide polyHIPE stabilized by surfactant, Pickering, and dual emulsifiers [60]. Scaffolds stabilized by Pickering particles exhibited slow release of AAO due to closed cellular morphology, while surfactant and dual emulsifier-stabilized HIPE templates exhibited an initial burst followed by slow release. Since the dual-emulsified Pickering HIPE template exhibited an improved modulus, the antibacterial activity of the dual-emulsified Pickering HIPE template was further investigated; the AAO-loaded scaffolds exhibited an inhibition zone of more than 4 mm for 2 weeks. Alternatively, Yang et al. produced a drug carrier HIPE template by mixing a solvent (dichloromethane), drug (enrofloxacin), and a polymer blend followed by solvent evaporation. The produced enrofloxacin polyHIPE exhibited fast and complete drug release, with 80 % of the drug released in 2.5 h, reaching 98 % within 10 h [166].

### 6.4. Other

Rarely reported applications and/or the features of prepared Pickering polyHIPEs will be reviewed in this section. Zhu et al. obtained a superhydrophobic Pickering polyHIPE when the particle with a single cavity was used as an HIPE stabilizer. The observed high water-contact angle (~152°) was attributed to rough pore surface due to embedded particles and the trapped air in pores as well as in the cavity of the particles [172]. Guan et al. reported superhydrophobic Pickering polyHIPEs with the WCA 162° [173]. The increased hydrophobicity was due to efficient post-modification of polyHIPE due to Si groups on the silica decorated pore surface, allowing tetraethyl orthosilicate (TEOS) and 1H,1H,2H,2H-perfluorooctyltrichlorosilane (FDTS) grafting on the pore surface. Another rarely reported application of Pickering polyHIPE is sound absorption. Liu et al. used Pickering polyHIPE as a sound absorber and reported it as an efficient low-frequency sound absorber due to its hierarchical porous structure, allowing higher surface area to contact air molecules and therefore, dissipate sound energy [174]. Additionally, electrically conducting composite Pickering polyHIPEs can be prepared by using $Ti_3AlC_2$ [175] and silver nanoparticles [58] paving the way for high surface electrodes for biosensor applications based on polyHIPEs.

## 7. Conclusion

Considering the emergence of Pickering polyHIPEs in 2007, the technique has found various applications within a relatively short timeframe. This is mainly due to the cost-effective and straightforward preparation of polyHIPEs, along with the unique features offered by Pickering polyHIPEs, such as their larger pores compared to conventional counterparts and their potential for functionalization during synthesis. With rapid advances in nanomaterials, such as MOFs, it is believed that the popularity of Pickering polyHIPEs will increase accordingly.

In this review, both the basics and advanced applications of Pickering polyHIPEs are examined, with a special focus on methods to achieve interconnected porous Pickering polyHIPEs. While Pickering polyHIPEs are being used in various applications, their range of use is limited due to their closed-cellular morphology. This is a drawback for applications requiring mass transfer. For instance, conventional polyHIPEs are widely used in tissue engineering applications. However, to best of our knowledge, there are no reports regarding the use of Pickering polyHIPEs as tissue engineering platforms. Therefore, unlocking the mechanism behind achieving interconnected Pickering polyHIPEs would unlock their full potential as well.

This review aims to provide directions for further research to demystify the mechanisms behind the formation of closed/open cellular porous forms of Pickering polyHIPEs. In fact, we believe that the challenge of achieving interconnected Pickering polyHIPEs is not due to its difficulty, but rather a lack of focused attention. Components of many observed open-porous Pickering polyHIPEs, such as commercially available monomers and particles, are readily accessible. Therefore, a simple library-based study comparing a few different monomers as the continuous phase and particles as stabilizers could either clarify the mechanism or provide important cues for further research. Once the mechanism for achieving interconnected porous Pickering polyHIPEs is established, their use is expected to increase significantly.

**CRediT authorship contribution statement**

**E. Durgut:** Writing – original draft, Visualization, Conceptualization. **F. Claeyssens:** Writing – review & editing, Supervision.

**Declaration of competing interest**

The authors declare that they have no known competing financial

interests or personal relationships that could have appeared to influence the work reported in this paper.

## Data availability

No data was used for the research described in the article.

## Acknowledgments

## References

[1] Silverstein MS. PolyHIPEs: recent advances in emulsion-templated porous polymers. Prog Polym Sci 2014;39:199–234. https://doi.org/10.1016/j.progpolymsci.2013.07.003.

[2] Cameron NR. High internal phase emulsion templating as a route to well-defined porous polymers. Polymer (Guildf) 2005;46:1439–49. https://doi.org/10.1016/j.polymer.2004.11.097.

[3] Aldemir Dikici B, Claeyssens F. Basic principles of emulsion templating and its use as an emerging manufacturing method of tissue engineering scaffolds. Front Bioeng Biotechnol 2020;8. https://doi.org/10.3389/fbioe.2020.00875.

[4] Low LE, Siva SP, Ho YK, Chan ES, Tey BT. Recent advances of characterization techniques for the formation, physical properties and stability of Pickering emulsion. Adv Colloid Interf Sci 2020;277:102117. https://doi.org/10.1016/j.cis.2020.102117.

[5] Albert C, Beladjine M, Tsapis N, Fattal E, Agnely F, Huang N. Pickering emulsions: preparation processes, key parameters governing their properties and potential for pharmaceutical applications. J Control Release 2019;309:302–32. https://doi.org/10.1016/j.jconrel.2019.07.003.

[6] Bago Rodriguez AM, Binks BP. High internal phase Pickering emulsions. Curr Opin Colloid Interface Sci 2022;57. https://doi.org/10.1016/j.cocis.2021.101556.

[7] Lissant KJ. The geometry of high-internal-phase-ratio emulsions. J Colloid Interface Sci 1966;22:462–8. https://doi.org/10.1016/0021-9797(66)90091-9.

[8] Wu R, Menner A, Bismarck A. Macroporous polymers made from medium internal phase emulsion templates: effect of emulsion formulation on the pore structure of polyMIPEs. Polymer (Guildf) 2013;54:5511–7. https://doi.org/10.1016/j.polymer.2013.08.029.

[9] Boyd J, Parkinson C, Sherman P. Factors affecting emulsion stability, and the HLB concept. J Colloid Interface Sci 1972;41:359–70. https://doi.org/10.1016/0021-9797(72)90122-1.

[10] Walstra P. Principles of emulsion formation. Chem Eng Sci 1993;48:333–49. https://doi.org/10.1016/0009-2509(93)80021-H.

[11] Ramsden W, Gotch F. Separation of solids in the surface-layers of solutions and 'suspensions' (observations on surface-membranes, bubbles, emulsions, and mechanical coagulation).—preliminary account. Proc R Soc Lond 1904;72:156–64. https://doi.org/10.1098/rspl.1903.0034.

[12] Pickering SU. Cxcvi.—emulsions. J Chem Soc Trans 1907;91:2001–21.

[13] Colver PJ, Bon SAF. Cellular polymer monoliths made via Pickering high internal phase emulsions. Chem Mater 2007;19:1537–9. https://doi.org/10.1021/cm0628810.

[14] Midmore BR. COLLOIDS AND a SURFACES preparation of a novel silica-stabilized oil/water emulsion. Colloids Surf A Physicochem Eng Asp 1998;132:257–65.

[15] Bizmark N, Ioannidis MA. Nanoparticle-stabilised emulsions: droplet armouring: vs. droplet bridging. Soft Matter 2018;14:6404–8. https://doi.org/10.1039/c8sm00938d.

[16] Arditty S, Whitby CP, Binks BP, Schmitt V, Leal-Calderon F. Some general features of limited coalescence in solid-stabilized emulsions. Eur Phys J E 2003;11:273–81. https://doi.org/10.1140/epje/i2003-10018-6.

[17] Pawar AB, Caggioni M, Ergun R, Hartel RW, Spicer PT. Arrested coalescence in Pickering emulsions. Soft Matter 2011;7:7710–6. https://doi.org/10.1039/c1sm05457k.

[18] Matter F, Luna AL, Niederberger M. From colloidal dispersions to aerogels: how to master nanoparticle gelation. Nano Today 2020;30:100827. https://doi.org/10.1016/j.nantod.2019.100827.

[19] Kim K, Kim S, Ryu J, Jeon J, Jang SG, Kim H, et al. Processable high internal phase Pickering emulsions using depletion attraction. Nat Commun 2017;8:1–8. https://doi.org/10.1038/ncomms14305.

[20] McClements DJ. Critical review of techniques and methodologies for characterization of emulsion stability. Crit Rev Food Sci Nutr 2007;47:611–49. https://doi.org/10.1080/10408390701289292.

[21] Ivanov IB, Danov KD, Kralchevsky PA. Flocculation and coalescence of micron-size emulsion droplets 1999;152:161–82.

[22] Meinders MBJ, Van Vliet T. The role of interfacial rheological properties on 2004;109:119–26. https://doi.org/10.1016/j.cis.2003.10.005.

[23] Binks BP, Kirkland M. Interfacial structure of solid-stabilised emulsions studied by scanning electron microscopy. Phys Chem Chem Phys 2002;4:3727–33. https://doi.org/10.1039/b110031a.

[24] Whitby CP, Wanless EJ. Controlling Pickering emulsion destabilisation: a route to fabricating new materials by phase inversion. Materials (Basel) 2016;9. https://doi.org/10.3390/ma9080626.

[25] Melle S, Lask M, Fuller GG. Pickering emulsions with controllable stability. Langmuir 2005;21:2158–62. https://doi.org/10.1021/la047691n.

[26] Aubry N. Destabilization of Pickering emulsions using external electric fields. 2010. p. 850–9. https://doi.org/10.1002/elps.200900574.

[27] Griffith C, Daigle H. Destabilizing Pickering emulsions using fumed silica particles with different wettabilities. J Colloid Interface Sci 2019;547:117–26. https://doi.org/10.1016/j.jcis.2019.03.048.

[28] Kumar H, Upendar S, Mani E, Madivala GB. Destabilization of Pickering emulsions by interfacial transport of mutually soluble solute. J Colloid Interface Sci 2023;633:166–76. https://doi.org/10.1016/j.jcis.2022.10.133.

[29] Foudazi R. HIPEs to PolyHIPEs. React Funct Polym 2021;164:104917. https://doi.org/10.1016/j.reactfunctpolym.2021.104917.

[30] Rajinder P. Yield stress and viscoelastic properties of high internal phase ratio emulsions. Colloid Polym Sci 1999;277:583–8. https://doi.org/10.1007/s003960050429.

[31] N. Sengokmen Ozsoz, S. Pashneh-Tala, F. Claeyssens, Optimization of a high internal phase emulsion-based resin for use in commercial vat photopolymerization additive manufacturing, 3D Print Addit Manuf (n.d.). doi: https://doi.org/10.1089/3dp.2022.0235.

[32] Sengokmen-Ozsoz N, Boston R, Claeyssens F. Investigating the potential of Electroless nickel plating for fabricating ultra-porous metal-based lattice structures using PolyHIPE templates. ACS Appl Mater Interfaces 2023;15:30769–79. https://doi.org/10.1021/acsami.3c04637.

[33] Gao H, Ma L, Cheng C, Liu J, Liang R, Zou L, et al. Review of recent advances in the preparation, properties, and applications of high internal phase emulsions. Trends Food Sci Technol 2021;112:36–49. https://doi.org/10.1016/j.tifs.2021.03.041.

[34] Menner A, Ikem V, Salgueiro M, Shaffer MSP, Bismarck A. High internal phase emulsion templates solely stabilised by functionalised titania nanoparticles. Chem Commun c 2007:4274–6. https://doi.org/10.1039/b708935j.

[35] Binks BP, Lumsdon SO. Catastrophic phase inversion of water-in-oil emulsions stabilized by hydrophobie silica. Langmuir 2000;16:2539–47. https://doi.org/10.1021/la991081j.

[36] Kralchevsky PA, Ivanov IB, Ananthapadmanabhan KP, Lips A. On the thermodynamics of particle-stabilized emulsions: curvature effects and catastrophic phase inversion. Langmuir 2005;21:50–63. https://doi.org/10.1021/la047793d.

[37] Aldemir Dikici B, Sherborne C, Reilly GC, Claeyssens F. Emulsion templated scaffolds manufactured from photocurable polycaprolactone. Polymer (Guildf) 2019;175:243–54. https://doi.org/10.1016/j.polymer.2019.05.023.

[38] Christenson EM, Soofi W, Holm JL, Cameron NR, Mikos AG. Biodegradable fumarate-based polyHIPEs as tissue engineering scaffolds. Biomacromolecules 2007;8:3806–14. https://doi.org/10.1021/bm7007235.

[39] Dunstan TS, Fletcher PDI, Mashinchi S. High internal phase emulsions: catastrophic phase inversion, stability, and triggered destabilization. Langmuir 2012;28:339–49. https://doi.org/10.1021/la204104m.

[40] Bizmark N, Du X, Ioannidis MA. High internal phase Pickering emulsions as templates for a cellulosic functional porous material. ACS Sustain Chem Eng 2020;8:3664–72. https://doi.org/10.1021/acssuschemeng.9b06577.

[41] Sun G, Li Z, Ngai T. Inversion of particle-stabilized emulsions to form high-internal-phase emulsions. Angew Chem 2010;122:2209–12. https://doi.org/10.1002/ange.200907175.

[42] Zhang T, Xu Z, Cai Z, Guo Q. Phase inversion of ionomer-stabilized emulsions to form high internal phase emulsions (HIPEs). Phys Chem Chem Phys 2015;17:16033–9. https://doi.org/10.1039/c5cp01157d.

[43] Chen Y, Wang Z, Wang D, Ma N, Li C, Wang Y. Surfactant-free emulsions with erasable triggered phase inversions. Langmuir 2016;32:11039–42. https://doi.org/10.1021/acs.langmuir.6b03189.

[44] Zou Y, Yang X, Scholten E. Tuning particle properties to control rheological behavior of high internal phase emulsion gels stabilized by zein/tannic acid complex particles. Food Hydrocoll 2019;89:163–70. https://doi.org/10.1016/j.foodhyd.2018.10.037.

[45] Song J, Sun Y, Wang H, Tan M. Preparation of high internal phase Pickering emulsion by centrifugation for 3D printing and astaxanthin delivery. Food Hydrocoll 2023;142:108840. https://doi.org/10.1016/j.foodhyd.2023.108840.

[46] Huang M, Wang J, Tan C. Tunable high internal phase emulsions stabilized by cross-linking/ electrostatic deposition of polysaccharides for delivery of hydrophobic bioactives. Food Hydrocoll 2021;118:106742. https://doi.org/10.1016/j.foodhyd.2021.106742.

[47] Malkin AY, Masalova I, Slatter P, Wilson K. Effect of droplet size on the rheological properties of highly-concentrated w/o emulsions. Rheol Acta 2004;43:584–91. https://doi.org/10.1007/s00397-003-0347-2.

[48] Pal R. Rheology of high internal phase ratio emulsions. Food Hydrocoll 2006;20:997–1005. https://doi.org/10.1016/j.foodhyd.2005.12.001.

[49] Welch CF, Rose GD, Malotky D, Eckersley ST. Rheology of high internal phase emulsions. Langmuir 2006;22:1544–50. https://doi.org/10.1021/la052207h.

[50] Foudazi R, Qavi S, Masalova I, Malkin AY. Physical chemistry of highly concentrated emulsions. Adv Colloid Interf Sci 2015;220:78–91. https://doi.org/10.1016/j.cis.2015.03.002.

[51] Arditty S, Schmitt V, Giermanska-Kahn J, Leal-Calderon F. Materials based on solid-stabilized emulsions. J Colloid Interface Sci 2004;275:659–64. https://doi.org/10.1016/j.jcis.2004.03.001.

[52] Kaganyuk M, Mohraz A. Role of particles in the rheology of solid-stabilized high internal phase emulsions. J Colloid Interface Sci 2019;540:197–206. https://doi.org/10.1016/j.jcis.2018.12.098.

[53] Langenfeld A, Schmitt V, Stébé MJ. Rheological behavior of fluorinated highly concentrated reverse emulsions with temperature. J Colloid Interface Sci 1999;218:522–8. https://doi.org/10.1006/jcis.1999.6427.

[54] Zou S, Yang Y, Liu H, Wang C. Synergistic stabilization and tunable structures of Pickering high internal phase emulsions by nanoparticles and surfactants. Colloids Surf A Physicochem Eng Asp 2013;436:1–9. https://doi.org/10.1016/j.colsurfa.2013.06.013.

[55] Williams JM, Gray AJ, Wilkerson MH. Emulsion stability and rigid foams from styrene or Divinylbenzene water-in-oil emulsions. Langmuir 1990;6:437–44. https://doi.org/10.1021/la00092a026.

[56] Levine S, Bowen BD, Partridge SJ. Stabilization of emulsions by fine particles I. Partitioning of particles between continuous phase and oil/water interface. Colloids Surf A Physicochem Eng Asp 1989;38:325–43. https://doi.org/10.1016/0166-6622(89)80271-9.

[57] Yi W, Wu H, Wang H, Du Q. Interconnectivity of macroporous hydrogels prepared via graphene oxide-stabilized Pickering high internal phase emulsions. Langmuir 2016;32:982–90. https://doi.org/10.1021/acs.langmuir.5b04477.

[58] Blancas Flores JM, Pérez García MG, González Contreras G, Coronado Mendoza A, Romero Arellano VH. Polydimethylsiloxane nanocomposite macroporous films preparedviaPickering high internal phase emulsions as effective dielectrics for enhancing the performance of triboelectric nanogenerators. RSC Adv 2020;11:416–24. https://doi.org/10.1039/d0ra07934k.

[59] Binks BP, Lumsdon SO. Pickering emulsions stabilized by monodisperse latex particles: effects of particle size. Langmuir 2001;17:4540–7. https://doi.org/10.1021/la0103822.

[60] Zou S, Wei Z, Hu Y, Deng Y, Tong Z, Wang C. Macroporous antibacterial hydrogels with tunable pore structures fabricated by using Pickering high internal phase emulsions as templates. Polym Chem 2014;5:4227–34. https://doi.org/10.1039/c4py00436a.

[61] Ikem VO, Menner A, Bismarck A. High internal phase emulsions stabilized solely by functionalized silica particles. Angew Chem 2008;120:8401–3. https://doi.org/10.1002/ange.200802244.

[62] Koroleva MY, Shirokikh SA, Zagoskin PS, Yurtov EV. Controlling pore sizes in highly porous poly(styrene-Divinylbenzene) sponges for preferable oil sorption. Polym Test 2019;77:105931. https://doi.org/10.1016/j.polymertesting.2019.105931.

[63] Viswanathan P, Johnson DW, Hurley C, Cameron NR, Battaglia G. 3D surface functionalization of emulsion-templated polymeric foams. Macromolecules 2014;47:7091–8. https://doi.org/10.1021/ma500968q.

[64] Yavuz E, Cherkasov N, Degirmenci V. Acid and base catalysed reactions in one pot with site-isolated polyHIPE catalysts. RSC Adv 2019;9:8175–83. https://doi.org/10.1039/c9ra01053j.

[65] Koler A, Paljevac M, Cmager N, Iskra J, Kolar M, Krajnc P. Poly(4-vinylpyridine) polyHIPEs as catalysts for cycloaddition click reaction. Polymer (Guildf) 2017;126:402–7. https://doi.org/10.1016/j.polymer.2017.04.051.

[66] Aldemir Dikici B, Malayeri A, Sherborne C, Dikici S, Paterson T, Dew L, et al. Thiolene-and Polycaprolactone methacrylate-based polymerized high internal phase emulsion (PolyHIPE) scaffolds for tissue engineering. Biomacromolecules 2022;23:720–30. https://doi.org/10.1021/acs.biomac.1c01129.

[67] Aldemir Dikici B, Chen MC, Dikici S, Chiu HC, Claeyssens F. In vivo bone regeneration capacity of multiscale porous polycaprolactone-based high internal phase emulsion (PolyHIPE) scaffolds in a rat calvarial defect model. ACS Appl Mater Interfaces 2023;15:27696–705. https://doi.org/10.1021/acsami.3c04362.

[68] Ansari H, Oladipo AA, Gazi M. Alginate-based porous polyHIPE for removal of single and multi-dye mixtures: competitive isotherm and molecular docking studies. Int J Biol Macromol 2023;246:125736. https://doi.org/10.1016/j.ijbiomac.2023.125736.

[69] Wang R, Li W, Lu R, Peng J, Liu X, Liu K, et al. A facile synthesis of cationic and super-hydrophobic polyHIPEs as precursors to carbon foam and adsorbents for removal of non-aqueous-phase dye. Colloids Surf A Physicochem Eng Asp 2020;605:125334. https://doi.org/10.1016/j.colsurfa.2020.125334.

[70] Mravljak R, Bizjak O, Podlogar M, Podgornik A. Effect of polyHIPE porosity on its hydrodynamic properties. Polym Test 2021;93. https://doi.org/10.1016/j.polymertesting.2020.106590.

[71] Hamann M, Quell A, Koch L, Stubenrauch C. On how the morphology affects water release of porous polystyrene. Mater Today Commun 2021;26:102087. https://doi.org/10.1016/j.mtcomm.2021.102087.

[72] Rouwkema J, Rivron NC, van Blitterswijk CA. Vascularization in tissue engineering. Trends Biotechnol 2008;26:434–41. https://doi.org/10.1016/j.tibtech.2008.04.009.

[73] Carnachan RJ, Bokhari M, Przyborski SA, Cameron NR. Tailoring the morphology of emulsion-templated porous polymers. Soft Matter 2006;2:608–16. https://doi.org/10.1039/B603211G.

[74] Barbetta A, Cameron NR. Morphology and surface area of emulsion-derived (PolyHIPE) solid foams prepared with oil-phase soluble porogenic solvents: three-component surfactant system. Macromolecules 2004;37:3202–13. https://doi.org/10.1021/ma035944y.

[75] Cameron NR, Sherrington DC. Preparation and glass transition temperatures of elastomeric PolyHIPE materials. J Mater Chem 1997;7:2209–12. https://doi.org/10.1039/a702030i.

[76] Hainey P, Huxham IM, Rowatt B, Sherrington DC, Tetley L. Synthesis and ultrastructural studies, of styrene-Divinylbenzene Polyhipe polymers. Macromolecules 1991;24:117–21. https://doi.org/10.1021/ma00001a019.

[77] Lovelady E, Kimmins SD, Wu J, Cameron NR. Preparation of emulsion-templated porous polymers using thiol-ene and thiol-yne chemistry. Polym Chem 2011;2:559–62. https://doi.org/10.1039/c0py00374c.

[78] Kramer S, Krajnc P, Pulko I. Influence of monomer structure, initiation, and porosity on mechanical and morphological characteristics of thiol-ene PolyHIPEs. Macromol Mater Eng 2023;308:1–7. https://doi.org/10.1002/mame.202300010.

[79] Palmer M, Hatley H. The role of surfactants in wastewater treatment: impact, removal and future techniques: a critical review. Water Res 2018;147:60–72. https://doi.org/10.1016/j.watres.2018.09.039.

[80] Aldemir Dikici B, Dikici S, Claeyssens F. Synergistic effect of type and concentration of surfactant and diluting solvent on the morphology of emulsion templated matrices developed as tissue engineering scaffolds. React Funct Polym 2022;180. https://doi.org/10.1016/j.reactfunctpolym.2022.105387.

[81] Zhou M, Bandegi A, Foudazi R. Control of pore interconnectivity in emulsion-templated porous polymers. Polymer (Guildf) 2023;281:126085. https://doi.org/10.1016/j.polymer.2023.126085.

[82] Hayek H, Rouxhet A, Abbad Andaloussi S, Kovačič S, Versace DL, Debuigne A. Quinizarin-based photoactive porous polymers from emulsion templates: monoliths versus membranes in photobactericidal applications. Eur Polym J 2024;217. https://doi.org/10.1016/j.eurpolymj.2024.113291.

[83] S. Kovačič, E. Žagar, C. Slugovc, Strength versus toughness of emulsion templated poly(Dicyclopentadiene) foams, Polymer (Guildf). 169 (2019) 58–65. doi:https://doi.org/10.1016/j.polymer.2019.02.045.

[84] Gurevitch I, Silverstein MS. Nanoparticle-based and organic-phase-based AGET ATRP polyHIPE synthesis within Pickering HIPEs and surfactant-stabilized HIPEs. Macromolecules 2011;44:3398–409. https://doi.org/10.1021/ma200362u.

[85] Zhang T, Cao H, Gui H, Xu Z, Zhao Y. Microphase-separated, magnetic macroporous polymers with amphiphilic swelling from emulsion templating. Polym Chem 2022;13:1090–7. https://doi.org/10.1039/d1py01584b.

[86] Kovačič NZ, Mazaj S, Ješelnik M, Pahovnik M, Žagar D, Slugovc E, et al. Synthesis and catalytic performance of hierarchically porous. Macromol Rapid Commun 2015;36:1605–11.

[87] Dhavalikar P, Shenoi J, Salhadar K, Chwatko M, Rodriguez-Rivera G, Cheshire J, et al. Engineering toolbox for systematic design of polyhipe architecture. Polymers (Basel) 2021;13. https://doi.org/10.3390/polym13091479.

[88] Hu Y, Gu X, Yang Y, Huang J, Hu M, Chen W, et al. Facile fabrication of poly(l -lactic acid)-grafted hydroxyapatite/poly(lactic- co -glycolic acid) scaffolds by Pickering high internal phase emulsion templates. ACS Appl Mater Interfaces 2014;6:17166–75. https://doi.org/10.1021/am504877h.

[89] Quell A, Sottmann T, Stubenrauch C. Diving into the finestructure of macroporous polymer foams synthesized via emulsion templating: a phase diagram study. Langmuir 2017;33:537–42. https://doi.org/10.1021/acs.langmuir.6b03762.

[90] Quell A, De Bergolis B, Drenckhan W, Stubenrauch C. How the locus of initiation influences the morphology and the pore connectivity of a monodisperse polymer foam. Macromolecules 2016;49:5059–67. https://doi.org/10.1021/acs.macromol.6b00494.

[91] Koch L, Drenckhan W, Stubenrauch C. Porous polymers via emulsion templating: pore deformation during solidification cannot be explained by an osmotic transport! Colloid Polym Sci 2021;299:233–42. https://doi.org/10.1007/s00396-020-04678-5.

[92] Koch L, Botsch S, Stubenrauch C. Emulsion templating: unexpected morphology of monodisperse macroporous polymers. J Colloid Interface Sci 2021;582:834–41. https://doi.org/10.1016/j.jcis.2020.08.106.

[93] Williams JM, Wrobleski DA. Spatial distribution of the phases in water-in-oil emulsions. Open and closed microcellular foams from cross-linked polystyrene. Langmuir 1988;4:656–62. https://doi.org/10.1021/la00081a027.

[94] Kim S, Kim JQ, Choi SQ, Kim K. Interconnectivity and morphology control of poly-high internal phase emulsions under photo-polymerization. Polym Chem 2022;13:492–500. https://doi.org/10.1039/d1py01175h.

[95] Cameron NR, Sherrington DC, Albiston L, Gregory DP. Study of the formation of the open-cellular morphology of poly(styrene/divinylbenzene) polyHIPE materials by cryo-SEM. Colloid Polym Sci 1996;274:592–5. https://doi.org/10.1007/BF00655236.

[96] Menner A, Bismarck A. New evidence for the mechanism of the pore formation in polymerising high internal phase emulsions or why polyHIPEs have an interconnected pore network structure. Macromol Symp 2006;242:19–24. https://doi.org/10.1002/masy.200651004.

[97] Durgut E, Sherborne C, Aldemir Dikici B, Reilly GC, Claeyssens F. Preparation of interconnected Pickering polymerized high internal phase emulsions by arrested coalescence. Langmuir 2022;38:10953–62. https://doi.org/10.1021/acs.langmuir.2c01243.

[98] Ikem VO, Menner A, Bismarck A. High-porosity macroporous polymers sythesized from titania-particle- stabilized medium and high internal phase emulsions. Langmuir 2010;26:8836–41. https://doi.org/10.1021/la9046066.

[99] Wong LLC, Ikem VO, Menner A, Bismarck A. Macroporous polymers with hierarchical pore structure from emulsion templates stabilised by both particles and surfactants. Macromol Rapid Commun 2011;32:1563–8. https://doi.org/10.1002/marc.201100382.

[100] Yang Y, Wei Z, Wang C, Tonga Z. Lignin-based Pickering HIPEs for macroporous foams and their enhanced adsorption of copper(II) ions. Chem Commun 2013;49: 7144–6. https://doi.org/10.1039/c3cc42270d.

[101] Pan J, Gao H, Zhang Y, Zeng J, Shi W, Song C, et al. Porous solid acid with high surface area derived from emulsion templating and hypercrosslinking for efficient one-pot conversion of cellulose to 5-hydroxymethylfurfural. RSC Adv 2014;4: 59175–84. https://doi.org/10.1039/c4ra10383a.

[102] Barbara I, Dourges MA, Deleuze H. Preparation of porous polyurethanes by emulsion-templated step growth polymerization. Polymer (Guildf) 2017;132: 243–51. https://doi.org/10.1016/j.polymer.2017.11.018.

[103] Ikem VO, Menner A, Horozov TS, Bismarck A. Highly permeable macroporous polymers synthesized from Pickering medium and high internal phase emulsion templates. Adv Mater 2010;22:3588–92. https://doi.org/10.1002/adma.201000729.

[104] Zhu W, Zhu Y, Zhou C, Zhang S. Pickering emulsion-templated polymers: insights into the relationship between surfactant and interconnecting pores. RSC Adv 2019;9:18909–16. https://doi.org/10.1039/c9ra03186c.

[105] Song IH, Kim DM, Choi JY, Jin SW, Nam KN, Park HJ, et al. Polyimide-based polyHIPEs prepared via pickering high internal phase emulsions. Polymers (Basel) 2019;11. https://doi.org/10.3390/polym11091499.

[106] Berezovska I, Kapilov K, Dhavalikar P, Cosgriff-Hernandez E, Silverstein MS. Reactive surfactants for achieving open-cell polyHIPE foams from pickering emulsions. Macromol Mater Eng 2021;306:1–8. https://doi.org/10.1002/mame.202000825.

[107] He H, Li W, Lamson M, Zhong M, Konkolewicz D, Hui CM, et al. Porous polymers prepared via high internal phase emulsion polymerization for reversible CO2 capture. Polymer (Guildf) 2014;55:385–94. https://doi.org/10.1016/j.polymer.2013.08.002.

[108] Yin D, Guan Y, Li B, Zhang B. Antagonistic effect of particles and surfactant on pore structure of macroporous materials based on high internal phase emulsion. Colloids Surf A Physicochem Eng Asp 2016;506:550–6. https://doi.org/10.1016/j.colsurfa.2016.06.060.

[109] Yin D, Li B, Liu J, Zhang Q. Structural diversity of multi-hollow microspheres via multiple Pickering emulsion co-stabilized by surfactant. Colloid Polym Sci 2015; 293:341–7. https://doi.org/10.1007/s00396-014-3401-y.

[110] Hua Y, Zhang S, Zhu Y, Chu Y, Chen J. Hydrophilic polymer foams with well-defined open-cell structure prepared from Pickering high internal phase emulsions. J Polym Sci Part A Polym Chem 2013;51:2181–7. https://doi.org/10.1002/pola.26588.

[111] Azhar U, Huyan C, Wan X, Zong C, Xu A, Liu J, et al. Porous multifunctional fluoropolymer composite foams prepared via humic acid modified Fe 3 O 4 nanoparticles stabilized Pickering high internal phase emulsion using cationic fluorosurfactant as co-stabilizer. Arab J Chem 2019;12:559–72. https://doi.org/10.1016/j.arabjc.2018.04.003.

[112] Woodward RT, De Luca F, Roberts AD, Bismarck A. High-surface-area, emulsion-templated carbon foams by activation of polyhipes derived from pickering emulsions. Materials (Basel) 2016;9. https://doi.org/10.3390/ma9090776.

[113] Vílchez A, Rodríguez-Abreu C, Menner A, Bismarck A, Esquena J. Antagonistic effects between magnetite nanoparticles and a hydrophobic surfactant in highly concentrated Pickering emulsions. Langmuir 2014;30:5064–74. https://doi.org/10.1021/la4034518.

[114] Shin H, Kim S, Han YK, Kim KH, Choi SQ. Preparation of a monolithic and macroporous superabsorbent polymer via a high internal phase Pickering emulsion template. J Appl Polym Sci 2019;136:1–7. https://doi.org/10.1002/app.48133.

[115] Zhu Y, Hua Y, Zhang S, Chen J, Hu CP. Vinyl ester oligomer crosslinked porous polymers prepared via surfactant-free high internal phase emulsions. J Nanomater 2012;2012. https://doi.org/10.1155/2012/307496.

[116] Xu H, Zheng X, Huang Y, Wang H, Du Q. Interconnected porous polymers with tunable pore throat size prepared via Pickering high internal phase emulsion. Langmuir 2016;32:38–45. https://doi.org/10.1021/acs.langmuir.5b03037.

[117] Yi F, Xu F, Gao Y, Li H, Chen D. Macrocellular polymer foams from water in oil high internal phase emulsion stabilized solely by polymer Janus nanoparticles: preparation and their application as support for Pd catalyst. RSC Adv 2015;5: 40227–35. https://doi.org/10.1039/c5ra01859e.

[118] Menner A, Verdejo R, Shaffer M, Bismarck A. Particle-stabilized surfactant-free medium internal phase emulsions as templates for porous nanocomposite materials: poly-Pickering-foams. Langmuir 2007;23:2398–403. https://doi.org/10.1021/la062712u.

[119] Tu S, Zhu C, Zhang L, Wang H, Du Q. Pore structure of macroporous polymers using polystyrene/silica composite particles as pickering stabilizers. Langmuir 2016;32:13159–66. https://doi.org/10.1021/acs.langmuir.6b03285.

[120] Durgut E, Zhou M, Dikici BA, Foudazi R, Claeyssens F. Modifying pickering polymerized high internal phase emulsion morphology by adjusting particle hydrophilicity. Colloids Surf A Physicochem Eng Asp 2024;680. https://doi.org/10.1016/j.colsurfa.2023.132629.

[121] Zheng X, Zhang Y, Wang H, Du Q. Interconnected macroporous polymers synthesized from silica particle stabilized high internal phase emulsions. Macromolecules 2014;47:6847–55. https://doi.org/10.1021/ma501253u.

[122] Zheng Z, Zheng X, Wang H, Du Q. Macroporous graphene oxide-polymer composite prepared through Pickering high internal phase emulsions. ACS Appl Mater Interfaces 2013;5:7974–82. https://doi.org/10.1021/am4020549.

[123] Pang B, Zhang H, Schilling M, Liu H, Wang X, Rehfeldt F, et al. High-internal-phase pickering emulsions stabilized by polymeric dialdehyde cellulose-based nanoparticles. ACS Sustain Chem Eng 2020;8:7371–9. https://doi.org/10.1021/acssuschemeng.0c01116.

[124] Zhang T, Xu Z, Guo Q. Closed-cell and open-cell porous polymers from ionomer-stabilized high internal phase emulsions. Polym Chem 2016;7:7469–76. https://doi.org/10.1039/c6py01725h.

[125] Hua Y, Chu Y, Zhang S, Zhu Y, Chen J. Macroporous materials from water-in-oil high internal phase emulsion stabilized solely by water-dispersible copolymer particles. Polymer (Guildf) 2013;54:5852–7. https://doi.org/10.1016/j.polymer.2013.08.055.

[126] Zhu Y, Huan S, Bai L, Ketola A, Shi X, Zhang X, et al. High internal phase oil-in-water Pickering emulsions stabilized by chitin nanofibrils: 3D structuring and solid foam. ACS Appl Mater Interfaces 2020;12:11240–51. https://doi.org/10.1021/acsami.9b23430.

[127] Zhu Y, Zhang R, Zhang S, Chu Y, Chen J. Macroporous polymers with aligned microporous walls from Pickering high internal phase emulsions. Langmuir 2016; 32:6083–8. https://doi.org/10.1021/acs.langmuir.6b00794.

[128] Silverstein MS, Tai H, Sergienko A, Lumelsky Y, Pavlovsky S. PolyHIPE: IPNs, hybrids, nanoscale porosity, silica monoliths and ICP-based sensors. Polymer (Guildf) 2005;46:6682–94. https://doi.org/10.1016/j.polymer.2005.05.022.

[129] Rohm K, Manas-Zloczower I, Feke D. Poly(HIPE) morphology, crosslink density, and mechanical properties influenced by surfactant concentration and composition. Colloids Surf A Physicochem Eng Asp 2019;583:123913. https://doi.org/10.1016/j.colsurfa.2019.123913.

[130] Barbetta A, Dentini M, Zannoni EM, De Stefano ME. Tailoring the porosity and morphology of gelatin-methacrylate polyHIPE scaffolds for tissue engineering applications. Langmuir 2005;21:12333–41. https://doi.org/10.1021/la0520233.

[131] Torquato ECC, Brito APN, Trovão RS, Oliveira MA, Smith NS, Pinto MCC, et al. Synthesis of porous polymeric supports with PolyHIPE structures based on styrene-Divinylbenzene copolymers. Macromol Symp 2020;394:1–7. https://doi.org/10.1002/masy.202000109.

[132] Luo Y, Wang AN, Gao X. Pushing the mechanical strength of PolyHIPEs up to the theoretical limit through living radical polymerization. Soft Matter 2012;8: 1824–30. https://doi.org/10.1039/c1sm06756g.

[133] Cameron NR, Sherrington DC. Synthesis and characterization of poly(aryl ether sulfone) PolyHIPE materials. Macromolecules 1997;30:5860–9. https://doi.org/10.1021/ma961403f.

[134] Golub D, Krajnc P. Emulsion templated hydrophilic polymethacrylates. Morphological features, water and dye absorption. React Funct Polym 2020;149: 104515. https://doi.org/10.1016/j.reactfunctpolym.2020.104515.

[135] Foudazi R, Zhao B, Gokun P, Manas-Zloczower I, Rowan SJ, Feke DL. The effect of shear on the evolution of morphology in high internal phase emulsions used as templates for structural and functional polymer foams. ACS Appl Polym Mater 2020;2:1579–86. https://doi.org/10.1021/acsapm.0c00003.

[136] Karaca I, Aldemir Dikici B. Quantitative evaluation of the pore and window sizes of tissue engineering scaffolds on scanning Electron microscope images using deep learning. ACS Omega 2024;9:24695–706. https://doi.org/10.1021/acsomega.4c01234.

[137] Riesco R, Boyer L, Blosse S, Lefebvre PM, Assemat P, Leichle T, et al. Water-in-PDMS emulsion templating of highly interconnected porous architectures for 3D cell culture. ACS Appl Mater Interfaces 2019;11:28631–40. https://doi.org/10.1021/acsami.9b07564.

[138] Munive-Olarte A, Hidalgo-Moyle JJ, Velasquillo C, Juarez-Moreno K, Mota-Morales JD. Boosting cell proliferation in three-dimensional polyacrylates/nanohydroxyapatite scaffolds synthesized by deep eutectic solvent-based emulsion templating. J Colloid Interface Sci 2022;607:298–311. https://doi.org/10.1016/j.jcis.2021.08.149.

[139] Yang S, Wang Y, Jia Y, Sun X, Sun P, Qin Y, et al. Tailoring the morphology and epoxy group content of glycidyl methacrylate-based polyHIPE monoliths via radiation-induced polymerization at room temperature. Colloid Polym Sci 2018; 296:1005–16. https://doi.org/10.1007/s00396-018-4307-x.

[140] Pulko I, Krajnc P. High internal phase emulsion templating - a path to hierarchically porous functional polymers. Macromol Rapid Commun 2012;33: 1731–46. https://doi.org/10.1002/marc.201200393.

[141] Owen R, Sherborne C, Paterson T, Green NH, Reilly GC, Claeyssens F. Emulsion templated scaffolds with tunable mechanical properties for bone tissue engineering. J Mech Behav Biomed Mater 2016;54:159–72. https://doi.org/10.1016/j.jmbbm.2015.09.019.

[142] Menner A, Haibach K, Powell R, Bismarck A. Tough reinforced open porous polymer foams via concentrated emulsion templating. Polymer (Guildf) 2006;47: 7628–35. https://doi.org/10.1016/j.polymer.2006.09.022.

[143] Huš S, Krajnc P. PolyHIPEs from methyl methacrylate: hierarchically structured microcellular polymers with exceptional mechanical properties. Polymer (Guildf) 2014;55:4420–4. https://doi.org/10.1016/j.polymer.2014.07.007.

[144] Ranting WU, Menner A, Bismarck A. Tough interconnected polymerized medium and high internal phase emulsions reinforced by silica particles. J Polym Sci Part A Polym Chem 2010;48:1979–89. https://doi.org/10.1002/POLA.23965.

[145] Haibach K, Menner A, Powell R, Bismarck A. Tailoring mechanical properties of highly porous polymer foams: silica particle reinforced polymer foams via emulsion templating. Polymer (Guildf) 2006;47:4513–9. https://doi.org/10.1016/j.polymer.2006.03.114.

[146] Azhar U, Huo Z, Yaqub R, Xu A, Zhang S, Geng B. Non-crosslinked fluorinated copolymer particles stabilized Pickering high internal phase emulsion for fabrication of porous polymer monoliths. Polymer (Guildf) 2019;172:160–9. https://doi.org/10.1016/j.polymer.2019.03.068.

[147] Jiang B, Wang Z, Zhao N. Effect of pore size and relative density on the mechanical properties of open cell aluminum foams. Scr Mater 2007;56:169–72. https://doi.org/10.1016/j.scriptamat.2006.08.070.

[148] Huš S, Kolar M, Krajnc P. Tailoring morphological features of cross-linked emulsion-templated poly(glycidyl methacrylate). Des Monomers Polym 2015;18: 698–703. https://doi.org/10.1080/15685551.2015.1070503.

[149] Li T, Liu H, Zeng L, Yang S, Li Z, Zhang J, et al. Macroporous magnetic poly (styrene-divinylbenzene) nanocomposites prepared via magnetite nanoparticles-stabilized high internal phase emulsions. J Mater Chem 2011;21:12865–72. https://doi.org/10.1039/c1jm10799b.

[150] Wang Q, Ma H, Chen J, Du Z, Mi J. Interfacial control of polyHIPE with nano-TiO2 particles and polyethylenimine toward actual application in CO2 capture. J Environ Chem Eng 2017;5:2807–14. https://doi.org/10.1016/j. jece.2017.05.034.

[151] Dupont H, Fouché C, Dourges MA, Schmitt V, Héroguez V. Polymerization of cellulose nanocrystals-based Pickering HIPE towards green porous materials. Carbohydr Polym 2020;243:116411. https://doi.org/10.1016/j. carbpol.2020.116411.

[152] Li X, Sun G, Li Y, Yu JC, Wu J, Ma GH, et al. Porous TiO2 materials through Pickering high-internal phase emulsion templating. Langmuir 2014;30:2676–83. https://doi.org/10.1021/la404930h.

[153] Zhu Y, Hua Y, Zhang S, Wang Y, Chen J. Open-cell macroporous bead: a novel polymeric support for heterogeneous photocatalytic reactions. J Polym Res 2015; 22. https://doi.org/10.1007/s10965-015-0703-9.

[154] Yüce E, Mert EH, Krajnc P, Parın FN, San N, Kaya D, et al. Photocatalytic activity of Titania/Polydicyclopentadiene PolyHIPE composites. Macromol Mater Eng 2017;302:1–8. https://doi.org/10.1002/mame.201700091.

[155] Lee J, Chang JY. A hierarchically porous catalytic monolith prepared from a Pickering high internal phase emulsion stabilized by microporous organic polymer particles. Chem Eng J 2020;381:122767. https://doi.org/10.1016/j. cej.2019.122767.

[156] Sun Y, Zhu Y, Zhang S, Binks BP. Fabrication of hierarchical macroporous ZIF-8 monoliths using high internal phase Pickering emulsion templates. Langmuir 2021;37:8435–44. https://doi.org/10.1021/acs.langmuir.1c00757.

[157] Gao H, Peng Y, Pan J, Zeng J, Song C, Zhang Y, et al. Synthesis and evaluation of macroporous polymerized solid acid derived from Pickering HIPEs for catalyzing cellulose into 5-hydroxymethylfurfural in an ionic liquid. RSC Adv 2014;4: 43209–38. https://doi.org/10.1039/c4ra06870j.

[158] Zhu Y, Wang W, Yu H, Wang A. Preparation of porous adsorbent via Pickering emulsion template for water treatment: a review. J Environ Sci (China) 2020;88: 217–36. https://doi.org/10.1016/j.jes.2019.09.001.

[159] Vrtovec N, Jurjevec S, Zabukovec Logar N, Mazaj M, Kovačič S. Metal oxide-derived MOF-74 polymer composites through Pickering emulsion-templating: interfacial recrystallization, hierarchical architectures, and CO2 capture performances. ACS Appl Mater Interfaces 2023;15:18354–61. https://doi.org/10.1021/acsami.3c01796.

[160] Lorignon F, Gossard A, Medjouel S, Carboni M, Meyer D. Controlling polyHIPE surface properties by tuning the hydrophobicity of MOF particles stabilizing a Pickering emulsion. ACS Appl Mater Interfaces 2023;15:30707–16. https://doi. org/10.1021/acsami.3c02987.

[161] Zhang T, Guo Q. Continuous preparation of polyHIPE monoliths from ionomer-stabilized high internal phase emulsions (HIPEs) for efficient recovery of spilled oils. Chem Eng J 2017;307:812–9. https://doi.org/10.1016/j.cej.2016.09.024.

[162] Abebe MW, Kim H. Methylcellulose/tannic acid complex particles coated on alginate hydrogel scaffold via Pickering for removal of methylene blue from aqueous and quinoline from non-aqueous media. Chemosphere 2022;286: 131597. https://doi.org/10.1016/j.chemosphere.2021.131597.

[163] Li X, Zhang T, Lu J, Xu Z, Zhao Y. Emulsion-templated, magnetic, hydrophilic–oleophobic composites for controlled water removal. Langmuir 2022;38:1422–31. https://doi.org/10.1021/acs.langmuir.1c02583.

[164] Cohen N, Silverstein MS. One-pot emulsion-templated synthesis of an elastomer-filled hydrogel framework. Macromolecules 2012;45:1612–21. https://doi.org/10.1021/ma2027337.

[165] Warwar Damouny C, Silverstein MS. Hydrogel-filled, semi-crystalline, nanoparticle-crosslinked, porous polymers from emulsion templating: structure, properties, and shape memory. Polymer (Guildf) 2016;82:262–73. https://doi.org/10.1016/j.polymer.2015.11.040.

[166] Yang T, Hu Y, Wang C, Binks BP. Fabrication of hierarchical macroporous biocompatible scaffolds by combining Pickering high internal phase emulsion templates with three-dimensional printing. ACS Appl Mater Interfaces 2017;9: 22950–8. https://doi.org/10.1021/acsami.7b05012.

[167] Gui H, Zhang T, Guo Q. Closed-cell, emulsionlated hydrogels for latent heat storage applications. Polym Chem 2018;9:3970–3. https://doi.org/10.1039/c8py00785c.

[168] Lu J, Zhang T, Xu Z, Yin X, Zhao Y. PolyHIPE composites for latent heat storage: flexibility and enhanced light to heat conversion. ACS Appl Polym Mater 2022;4: 8083–91. https://doi.org/10.1021/acsapm.2c01027.

[169] Li B, Chen Q, Dong G, Yin D. Close-cellar shape-stable phase change material monolith prepared by high internal phase Pickering emulsion polymerization. Compos Part A Appl Sci Manuf 2022;163:107143. https://doi.org/10.1016/j. compositesa.2022.107143.

[170] Rosen N, Toledo H, Silverstein MS. Encapsulating an inorganic phase change material within emulsion-templated polymers: thermal energy storage and release. Polymer (Guildf) 2023;276:125947. https://doi.org/10.1016/j. polymer.2023.125947.

[171] Yin X, Zhang T, Zhao T, Wang K, Xu Z, Zhao Y. Cellulose-based, flexible polyurethane polyHIPEs with quasi-closed-cell structures and high stability for thermal insulation. Carbohydr Polym 2023;302:120385. https://doi.org/10.1016/j.carbpol.2022.120385.

[172] Zhu Y, Zhang S, Hua Y, Zhang H, Chen J. Synthesis of latex particles with a complex structure as an emulsifier of pickering high internal phase emulsions. Ind Eng Chem Res 2014;53:4642–9. https://doi.org/10.1021/ie404009x.

[173] Guan X, Ngai T. PH-sensitive W/O Pickering high internal phase emulsions and W/O/W high internal water-phase double emulsions with tailored microstructures Costabilized by lecithin and silica inorganic particles. Langmuir 2021;37:2843–54. https://doi.org/10.1021/acs.langmuir.0c03658.

[174] Liu J, Wang P, He Y, Liu K, Miao R, Fang Y. Polymerizable nonconventional gel emulsions and their utilization in the template preparation of Low-density, high-strength polymeric monoliths and 3D printing. Macromolecules 2019;52: 2456–63. https://doi.org/10.1021/acs.macromol.8b02610.

[175] Zheng Z, Zhao Y, Ye Z, Hu J, Wang H. Electrically conductive porous MXene-polymer composites with ultralow percolation threshold via pickering high internal phase emulsion templating strategy. J Colloid Interface Sci 2022;618: 290–9. https://doi.org/10.1016/j.jcis.2022.03.086.